Aus dem Experimental and Clinical Research Center (ECRC)
der Medizinischen Fakultät Charité –Universitätsmedizin Berlin

DISSERTATION

Rollen des perivaskulären Fettgewebes und der spannungsabhängigen K_V7-Kaliumkanäle im Gefäßtonus

Roles of Perivascular Adipose Tissue and K_V7 Voltage-dependent Potassium Channels in Vascular Tone

zur Erlangung des akademischen Grades
Doctor medicinae (Dr. med.)

vorgelegt der Medizinischen Fakultät
Charité – Universitätsmedizin Berlin

Von

Yibin Wang
aus Jiangsu, China

Datum der Promotion: 25.06.2023

Table of Contents

List of abbreviations

PVAT	perivascular adipose tissue
VSMC	vascular smooth muscle cell
PVATRF	perivascular adipose tissue-derived relaxing factor
ADRF	adipocyte-derived relaxing factor
PE	phenylephrine
5-HT	serotonin
PSS	physiological saline solution
GO	Gene Ontology
DO	Disease Ontology
KEGG	Kyoto Encyclopedia of Genes and Genomes
COX	cyclooxygenase
PG	particular prostaglandin
CYP	cytochrome P450
PGC-1α	peroxisome proliferator-activated receptor γ co-activator 1α

Abstract

Hypertension is widely acknowledged as a major risk factor in the progression of many vascular diseases, especially for elderlies. The vascular tone plays a key role in several major areas of research.

The K_V7 voltage-dependent potassium channels (also known as K_V7 channels) are encoded by the KCNQ genes. The relationships between perivascular adipose tissue (PVAT) and K_V7 channels are still unclear. First, the role of PVAT in mouse mesenteric artery relaxation was examined. Aging, as well as other physiological changes, affects PVAT. K_V7 channels and the relative modulators are studied mainly on a mouse model in our research. Wire myography and membrane potential experiments were used to evaluate the vascular function in vitro. RNA sequencing experiments and q-PCR helped to reveal the roles of potential pathways influencing artery tone. The data indicates that the tone of the mesenteric artery is suppressed by the activation of K_V7 channels in young mouse. K_V7 channels participated in regulation not only through metabolic processes, but also through perivascular adipose tissue-derived relaxation factors. As a novel pharmacological vasodilator, QO58 can open the KCNQ channels in mouse mesenteric arteries, that reduced depolarization caused by α1 adrenoceptor agonist. This reduction was reversed by XE991, a K_V7 channel blocker. The results demonstrated studying aging and K_V7 voltage-dependent potassium channels might lead to innovative ways to treat vascular dysfunction. Ultimately, K_V7 channels indicate a prospective therapeutic in the field of aging research and hypertension treatment.

Zusammenfassung

Bluthochdruck ist ein Haupt-Risikofaktor für die Entwicklung vieler Herz-Kreislauf-Erkrankungen, insbesondere im Alter. Dem Gefäßtonus kommt eine wichtige Rolle in verschiedenen Hauptforschungsbereichen zu.

Die spannungsregulierten K_V7-Kalium-Kanäle (K_V7-Kanäle) werden durch KCNQ-Gene codiert. Die Zusammenhänge zwischen perivaskulärem Fettgewebe (perivascular adipose tissue, PVAT) und K_V7-Kanälen sind noch unklar. Zuerst wurde die Bedeutung von PVAT bei der Relaxation von Mesenterialarterien der Maus untersucht. Alter, ebenso wie weitere physiologische Veränderungen, beeinflusst PVAT. K_V7-Kanäle und ihre Modulatoren wurden hauptsächlich im Mausmodell studiert. Draht-Myographie und Membranpotential-Messungen wurden durchgeführt, um die Gefäßfunktion in vitro zu beurteilen. RNA-Sequenzierung und q-PCR-Experimente unterstützten das Aufdecken der Rolle möglicher Signalwege mit Einfluss auf den arteriellen Gefäßtonus. Die Daten weisen darauf hin, dass der Tonus der Mesenterialarterien durch Aktivierung spannungsabhängiger K_V7-Kalium-Kanäle bei jungen Mäusen vermindert wird. K_V7-Kanäle beeinflussen diese Regulation nicht nur durch metabolische Prozesse, sondern auch über Faktoren aus dem perivaskulärem Fettgewebe. Als neuartiger pharmakologischer Vasodilatator kann QO58 die KCNQ-Kanäle in mesenterialen Arterien der Maus öffnen, wodurch die α-1-Adrenozeptor-Agonisten-vermittelte Depolarisation reduziert wurde. Diese Verringerung wurde durch den K_V7-Kanal-Blocker XE991 rückgängig gemacht. Unsere Daten zeigen, dass die Untersuchung von Alterung und K_V7-Kanälen innovative Behandlungswege für vaskuläre Dysfunktion aufzeigen könnte. Schließlich stellen K_V7-Kanäle ein vielversprechendes Ziel in der Altersforschung und der Behandlung von Bluthochdruck dar.

1. Introduction

Hypertension is known as the major risk factor for cardiovascular disease. It causes dysfunction in human body through a complex change regarding cardiac, vascular, renal, and neuralhormonal system. Various researches suggested that vascular dysfunction is the main factor causing extensive morbidity and mortality due to many cardiovascular diseases, especially hypertension, and atherosclerosis (*1, 2*).

As for elderly patients, it is even more challenging to control the blood pressure, as for previous research, aging is reported to be another independent factor that influences the adjustment of vascular tone. About 80% elderlies above 80 years old suffer from aging-associated hypertension (*3*).

As hypertension is a multi-factorial disorder, it may be caused by the changing of the vascular tone. The underlying process of vascular tone regulation is still not clear, but it may involve vascular structure remodeling, vascular calcification, and chemoreceptor changing. However, the blood pressure controlling disorders caused by aging are reported to be related to mineralocorticoid receptors in vascular smooth muscle cells (VSMCs), that is proved not related to any vascular structure changing (*4*). Vascular calcification is another important cause that affects the survival rate in chronic vascular disease, combining negative effects of refractory hypertension (*5*). In some cases, the anti-contractile function of endothelial vasodilator is attenuated in vascular smooth muscle cells. It is reported to be one reason that causes hypertension, which is also recognized as the hyper-contractile state (*6, 7*). Alternatively, the internal abnormalities of renal vascular smooth muscle cells may alter renal vascular tone and perfusion, which will lead to a recognized change in renal processing salt, thereby promoting and/or maintaining elevated blood pressure. Another aspect is that, dysfunction of peripheral resistance arteries can be the risk factor of cardiovascular disease (*8*). However, in either case, it is essential to focus on the dysfunction in the key VSMC protein that regulates the state of cell contraction, that could bring different diagnostic and therapeutic targets to humanbeings.

Perivascular adipose tissue (PVAT) is reported to be a promising target which regulates the vascular dysfunction in pathophysiological conditions (*9*). The aorta and its branches are surrounded by PVAT. The anti-contractile effect of PVAT is widely studied (*10*). PVAT has been reported widely as anti-contractile part related to the opening of potassium channels in VSMCs (*11*). In addition, various lipids and FAs are related to PVAT. The development of treatments for cardiovascular and kidney diseases has taken a step further lately involving the research on fatty acids. PVAT is now known as a paracrine organ (*12*). On one hand, PVAT provides mechanical protection to vessels. On the other hand, PVAT also releases perivascular adipose tissue-derived relaxing factors (PVATRFs). Among PVATRFs, the transferable adipocyte-derived relaxing factor (ADRF) is one that draws my attention that has the inhibition effect on the vascular contraction pre-induced by phenylephrine (PE), serotonin (5-HT), and angiotensin II (*13*).

Potassium channels are reported to play important functions regarding lipid microenvironment of cellular membrane in previous research (*14*). The K_V7 voltage-dependent potassium channels (also known as K_V7 channels) are encoded by the KCNQ gene. XE991 is widely used in rat and mouse aorta and mesenteric arteries as a specific K_V7 channel blocker, former research revealed that the PVAT has anti-contractile effects

which could be abolished by XE991 (*15*).

For deeper understanding of KCNQ channels, a compound 5-(2,6-Dichloro-5-fluoro-3-pyridinyl)-3-phenyl-2-(trifluoromethyl)-pyrazolo[1,5-a]pyrimidin-7(4H)-one (known as QO58) is used as selectively activator KCNQ/M-channels (*16-18*). QO58 shows a different mechanism of action from the known Kv7 openers, confirmed with a whole-cell patch-clamp recording study (*17*). For a better lipophilicity and hydrophilicity, QO58-lysine, a similar compound was synthesized based on QO58 (*17*), moreover, the in-vivo bioavailability of intravenous experiment was also performed without exhibiting obvious toxic effects. The function of K_V7 channels was studied with these two compounds in mesenteric arteries. It is confirmed in the previous study of Maik Gollasch et al. that PVAT play a key role in anti-contractile effect in mesenteric arteries, especially in young mice (*19*). Therefore, it is still not clear if aging is an independent factor attenuating the anti-contractile effect of PVAT, and how K_V7 channels are involved.

2. Aims and Hypotheses

The main purpose of the project was to reveal the roles of the adipose tissue and K_V7 voltage-dependent potassium channels in vascular tone. The hypotheses below were studied:

2.1 Hypothesis #1

The present study aimed to examine the control of mesenteric arterial tone and its relationship with age, and whether the selectivities of QO58 and QO58-lysine are different. To test this hypothesis, mesenteric arteries (both with and without PVAT) from wild-type mice and α1 adrenoceptor agonist (phenylephrine or methoxamine) were used to determine whether anti-contractile effects of PVAT are different.

2.2 Hypothesis #2

The present study aimed to examine whether the change of anti-contractile effect is related to perivascular adipose tissue. To test this hypothesis, wire myography was performed to determine the anti-contractile effect of PVAT.

2.3 Hypothesis #3

The present study aimed to examine how K_V7 channels play a role in the regulation mesenteric artery contraction. To test this hypothesis, membrane potential recordings, quantitative real-time PCR, and RNA-sequencing were performed to determine whether K_V7 channels are related to the dysfunction of the mesenteric artery tone caused by aging.

3. Methods

3.1 Animal preparation.

Male mice were mainly used in this research. The experimental animals were all raised and fed within standard conditions. The mice were kept under a 12-hour, day-night cycle system, and they had open access to press feed (0.25% sodium, SNIFF Specialties GmbH, Soest) and also water. Animal care were in accordance with American Physiological Society guidelines, and local authorities (Landesamt für Gesundheit und Soziales Berlin, LAGeSo) approved all protocols. Wild-type mice (C57BL/6N) were used with different age from 8 weeks to 24 months, and the selected animals were painlessly killed by cervical dislocation after anesthesia with isoflurane. Mesenteric tissue was taken from mice afterwards. Intestine was separated from mesenteric arteries after cutting open the abdominal wall of the mouse. The mesenteric arteries and perivascular adipose tissue were put in a Petri dish with physiological saline solution (PSS). The protocol of PSS is as following: 119 mmol/L NaCl, 4.7 mmol/L KCl, 1.2 mmol/L KH_2PO_4, 25 mmol/L $NaHCO_3$, 1.2 mmol/L Mg_2SO_4, 11.1 mmol/L glucose, 1.6 mmol/L $CaCl_2$) at 4°C. And then some part of the connecting tissue were removed and the blood on the surface of the tissue were washed out under a stereo microscope (Nikon, SMZ645). The mesenteric arteries with PVAT were taken for further experiments. The first and second order were cut off and they were used for myoghraphy and membrane potential test.

For experiments on the mice of different age, 11 to 18-weeks old mice were defined as young group, 50 to 54-weeks-old mice were defined as 12-month-old group, 66 to 69-weeks-old mice were defined as 16-month-old group, and 105 to 106-weeks-old mice were defined as 24-month-old group. All experiments were done according to the animal protection German legislation.

3.2 Wire Myography.

Mice were sacrificed with isoflurane anaesthesia. Mouse mesenteric arteries were dissected using microscope right after the mouse was sacrificed. All the steps below were kept in the cold (4°C), oxygenated (95% O_2/5% CO_2) PSS. The PSS was changed every 20 minutes. The whole plate were put under the stereo microscope (Nikon, SMZ645).

The samples were dissected into 2 mm out of the vessels without damaging adventitia. (+) PVAT group represented those with perivascular adipose tissue, and the (–) PVAT rings were those without perivascular adipose tissue and connective tissue. 5mL organ bath was filled with oxygenated PSS and put on a Mulvany Small Vessel Myograph (DMT 610 M; Danish Myo Technology, Denmark). Two wires were inserted into each artery. The wires were fixed on the chambers inside the organ bath. The wires should be of 0.0394 mm diameter and stainless steel. After fixing the wires, organ bath was kept warm at 37°C. After 30 to 60 minutes, vessels were normalized of which the passive diameters were at 100 mm Hg. The normalization of all mesenteric rings were done under a tension equivalent to 0.9 times the diameter of the vessel at 100 mm Hg, using LabChart DMT normalizing module (*12, 20*). The data acquisition was performed and displayed after

normalization using LabChart5 (a software from AD Instruments Ltd. Spechbach, Germany). 30 minutes after normalization, the mesenteric rings were pre-contracted with an isotonic external composition of 60 mM KCl or 1–3 μM α1 adrenoceptor agonist (phenylephrine or methoxamine). Then a resting tension was acquired when the tension was stable longer than five minutes. The 60 mM KCl solution contains 63.7 mmol/L NaCl, 60 mmol/L KCl, 1.2 mmol/L KH_2PO_4, 25 mmol/L $NaHCO_3$, 1.2 mmol/L Mg_2SO_4, 11.1 mmol/L glucose and 1.6 mmol/L $CaCl_2$ (*20*). After the resting tension was recorded for above 2 minutes, the KCl solution was washed out for three times with warm oxygenated PSS at 37°C. 30 minutes after washing, subsequent drugs were added into the chambers according to protocol. This washing step was not taken in those groups during which KCl was not used. The tension was presented in the results and figures using the percentage of the steady-state tension recorded with KCl or with α1 adrenoceptor agonist.

3.3 Membrane potential recordings.

The mesenteric arteries were prepared with the similar way of wire myography, and the materials were isolated immediately after sacrificing with isoflurane anaesthesia. All the steps below should be in the cold (4°C), oxygenated (95% O_2/5% CO_2) PSS (with the same formula as described above). The mesenteric artery was dissected into 2 mm, and two stainless steel wires were inserted into the ring. The mesenteric artery ring was fixed in a oxygenated (95% O_2/5% CO_2, pH 7.4) 10 mL organ bath filled with PSS. PSS bath was kept warm at 37°C. Vessels were normalized of which the passive diameters were at 100mm Hg.

Microelectrodes were made by pulling from aluminosilicate glass before the next steps. 30 minutes after normalization, the microelectrode was filled with 3 mol/L KCl. The microelectrode was lightly and slowly moved using a micromanipulator (UMP, Sensapex), until it impaled on the adventitial side of the vessel.

Intracellular recordings of membrane potential was made with an amplifier (DUO 773, World Precision Instruments). Some basic rules were applied for acceptance: (a) a cell penetration should cause a sudden change in membrane potential; (b) the resistance should be constantly recorded before and after the cell penetration; (c) the recording should be at least 1 min; (d) the base line should not be changed after removing the electrode (*21*).

3.4 Quantitative real-time PCR.

Organs were collected using dry ice, then stored at −80 °C until further used immediatedly after the mice were sacrificed. Mesenteric arteries (first branches) and PVAT were isolated from young (11 to 18-weeks-old), 12-months-old, 16- months-old, and 24-month-old mice. The RNeasy RNA isolation kit from Qiagen company (Qiagen, Germantown, MD) was used for extracting total RNA from all groups of samples at the same time, based on the protocol from the website of Qiagen. Disruption and homogenization of tissue were carried out rapidly afterwards. The concentration and OD value (260/ 280) were tested using the NanoDrop-1000 spectrophotometer (*21*). All related experiments were taken on dry ice. 2mg RNA was taken for the following

cDNA transcription. The PCR tests were performed on Biosystems 7500 Fast Real-Time PCR System (Life Technologies Corporation, Carlsbad, CA, USA). The running cycling accords to the manufacturer's instructions. The working mixture was activated at 95°C for 10 minutes and then 40 cycles were made using 95°C for 15 seconds and 60°C for 1 minute (*21*). All the experimental groups and negative control groups were performed in parallel. All primers were synthesized by BioTez (Berlin, Germany), and based on following sequences. The relative standard curve was used approach to assess the KCNQ mRNA expression obtained by quantitative real-time PCR. The expression of 18s was used for normalization of target gene expression, and the primer for 18s is also listed below. The expression of 18s as a reference gene did not alter between young and aged mouse tissues under our experimental circumstances. The 2Ct technique was used to determine the fold change in gene expression between young and aged mice. (*21*).

The following primers were used:

18s: F: 5'-ACATCCAAGGAAGGCAGCAG-3';

R: 5'-TTTTCGTCACTACCTCCCCG-3'.

Kcnq1: F: 5'-AGCAGTATGCCGCTCTGG-3';

R: 5'-AGATGCCCACGTACTTGCTG-3'.

Kcnq3: F:5'-CAGTATTCGGCCGGACATCT-3';

R:5'-GAGACTGCTGGGATGGGTAG-3'.

Kcnq4: F:5'-CACTTTGAGAAGCGCAGGAT-3';

R:5'-CCAGGTGGCTGTCAAATAGG-3'.

Kcnq5: F:5'-CCTCACTACGGCTCAAGAGT-3';

R:5'-TTAAGTGGTGGGGTGAGGTC-3'.

3.5 RNA Sequencing.

Organs were collected immediately after sacrificing mice, and stored at −80 °C until further used. Mesenteric arteries (first branches) and PVAT were isolated using the same protocol addressed above in 3.4. The same kit used to extract total RNA was also same as described above in 3.4. Dry ice was used in the whole experiment and for transporting to keep the low temperature.

RNA-seq was done on the Illumina Genome Analyzer Novaseq 6000 platform under Agilent 2100 bioanalyzer quality control. The DESeq2 R package version 1.20.0 was used to perform differential expression analysis (*22*). The clusterProfiler was used for enrichment analysis, including Gene Ontology (GO) Enrichment, Disease Ontology (DO) Enrichment, Kyoto Encyclopedia of Genes and Genomes (KEGG) and Reactome database Enrichment (*23*). The heat map was generated with the Morpheus software (https://software.broadinstitute.org/morpheus) (*21*).

3.6 Materials.

The involved chemicals used in experiments were acquired from Sigma-Aldrich (Munich, Deisenhofen or Schnelldorf, Germany) and Merck (Darmstadt, Germany). As a solvent to QO58 and QO58-lysine, DMSO was used beblow 0.5% in the final concerntration. DMSO is demonstrated in results for not having influence on the arterial tone (*21*). Drugs were freshly dissolved in DMSO or physiological saline solution based on the material sheet, and it is performed on the same day of each experiment. The final concentration of substances were used as written in the protocols: phenylephrine (Sigma Aldrich) and methoxamine (Sigma Aldrich) ranged from 0.01 to 100 µmol/L; retigabine (Valeant Research North America) ranged from 10 nmol/L to 100 µmol/L, flupirtine (Tocris) ranged from 10 nmol/L to 100 µmol/L, QO58 (Tocris) ranged from 0.01 to 30 µmol/L, QO58-lysine ranged from 10 nmol/L to 30 µmol/L; 3 µmol/L XE991 (Tocris).

3.7 Statistical analysis.

Datas and results were shown as mean ± SEM or ± SD in the graphs using GraphPad Prism version 5.0 (GraphPad Software, La Jolla, California, USA). EC50 values were calculated with a Hill equation: $T = (B0 – Be) / (1 + ([D]/EC50)n) + Be$. In which the T is the relative tension after applying the substance (D). Be is the maximum response after applying the drug. B0 is a constant. EC50 reffers to the concentration of the drug that elicits a half-maximal response. GraphPad Prism version 5.0 (GraphPad Software, California, USA) software was used to curve fitting procedure. Mann-Whitney test, nonparametric t-test and nonparametric ANOVA (Kruskal-Wallis test) were used to display the statistical significance in the statistics. Results with the P values < 0.05 were determined statistically significant. In the results and published manuscripts, the N is the number of animals, and n is the number of artery rings. All figures were merged with CorelDRAW Graphics Suite software (Ottawa, Canada).

A complete descriptions of methods can be found in:

Yibin Wang, Fatima Yildiz, Andrey Struve, Mario Kassmann, Lajos Markó, May-Britt Köhler, Friedrich C. Luft, Maik Gollasch and Dmitry Tsvetkov. Aging affects K_V7 channels and perivascular-adipose tissue-mediated vascular tone. Front. Physiol., 26 November 2021; 12:749709.

DOI link: https://doi.org/10.3389/fphys.2021.749709.

A copy of this publication is attached.

4. Results

This chapter contains my main findings in the publication on Frontiers in Physiology. The amount of animals is represented by N, whereas the amount of vessels is represented by n.

4.1 PVAT has the anti-contractile effect in WT mice.

As an α1-adrenoceptor agonist, methoxamine (ME) contracted isolated mesenteric arteries in WT young mice (around 12 to 16-weeks-old). To test if PVAT has the anticontractile effect, wire myography experiments were done on mesenteric arteries from young mice with and without PVAT. With a concentration gradient of α1 adrenoceptor agonist methoxamine from $1*10^{-8}$ to $3*10^{-5}$ mol/L, the tension of mesenteric artery rings was increasing (Figure. 1A*). The concentration-response relationships between methoxamine and artery tension were measured both in (−) PVAT (n = 10, N = 5) and (+) PVAT (n = 10, N = 4) mesenteric arteries (Figure. 1B*). PVAT showed a significant anticontractile effect in mesenteric arteries of young mice. Notably, concentration-response curve for tension of (+) PVAT artery samples showed a right shift comparing to those of (-) PVAT ones. *$p < 0.05$ by two-way ANOVA followed by Bonferroni post hoc test.

4.2 Age variations in the PVAT of the wild-type mice.

Another series of experiments were done on mesenteric arteries from old mice with and without PVAT. It showed α1-adrenoceptor agonist induced similar contractions in both groups with and without PVAT (Figure. 1C*). In 12-months-old group, the concentration-response relationships between methoxamine and artery tension showed no significant difference between (−) PVAT (n = 6, N = 2) and (+) PVAT (n = 9, N = 2) mesenteric arteries (Figure. 1D*). The result was confirmed also in 16 months old group (Figure. 1E*), the concentration-response relationships between methoxamine and artery tension showed no significant difference between (−) PVAT (n = 7, N = 3) and (+) PVAT (n = 9, N = 3) mesenteric arteries (Figure. 1F*). P>0.05, statistics were confirmed by two-way ANOVA followed by Bonferroni post hoc test. The results shows anticontractile effect of PVAT are impaired in the WT aged mice older than 12-months-old.

4.3 K_V7 is proved to be involved in anti-contractile effect, using the opener of K_V7 channel.

The involvement of K_V7 channels in aging was investigated, the K_V7 channel openers (both flupirtine and retigabine) were used to relax the mesenteric arteries of WT young mice, after pre-contracted by an α1 adrenoceptor agonist phenylephrine. Flupirtine caused concentration-dependent relaxations in (-) PVAT mesenteric arteries of young mice (Figure. 2A*). While in (-) PVAT mesenteric arteries from 24-months-old mice, the relaxations showed attenuated, and the change was significant (Figure. 2B*). Retigabine also caused concentration-dependent relaxations in (-) PVAT mesenteric arteries from young mice (n = 12, N = 3)

(Figure. 2C*). While in (-) PVAT mesenteric arteries from 24 months old mice (n = 7, N = 2), the relaxations were reduced, and the change was significant (Figure. 2D*).

Other two important substances named QO58 and QO58-lysine were also used in our study as K_V7 channel openers.

Concentration-dependent relaxations were also caused by QO58 and QO58-lysine in (-) PVAT mesenteric arteries from young mice (Figure. 3A, C*). QO58-induced relaxation was attenuated after pre-incubation with 3 μm XE991 (n = 10, N = 4) comparing in the absence of XE991 (n = 6, N = 3) (Figure. 3B*). QO58-lysine-induced relaxation was not significantly attenuated after pre-incubation with 3 μm XE991 (n = 10, N = 4) comparing in the absence of XE991 (n = 9, N = 3) (Figure. 3D*).

However the relaxation effect was suppressed in the control group using aged mice of 16-months-old (n = 13, N = 2) comparing young mice (n = 11, N = 2) (Figure. 3E*).

4.4 Function of K_V7 channels in young mice mesenteric arteries repolarization after depolarization caused by α1 agonist.

Membrane potential detecting was used to reveal the role of K_V7 channels. The application of the α1 adrenoceptor agonist methoxamine (3μmol/L) induced depolarization of cellular membrane in mesenteric artery. In mesenteric artery from young mouse, a repolarization was seen after adding 3μmol/L QO58, and the repolarization can be reversed by 3μM XE991, *$p<0.05$ statistics were confirmed by One-way ANOVA test with post-hoc Dunn's multiple comparison test (n = 7, N = 7) (Figure. S1 D, E*).

However, in mesenteric artery from old mouse, no significant repolarization was seen after adding 3μmol/L QO58, (n = 5, N = 5) (Figure. S1 F, G*).

In young mice, relaxation induced by QO58 was also reversed by XE991, consistent with the above.

4.5 Attenuated anti-contractile effect in aged mice is not related to the expression of K_V7 channels.

After showing that voltage-dependent potassium channels v in the attenuating of PVAT effect of aged mice, qPCR tests were performed on mesenteric arteries of young mice, 12-months-old mice, 16-months-old mice and 24-months-old mice, the mRNA level of *Kcnq1, Kcnq3, Kcnq4, Kcnq5* was not significantly changed due to aging (Figure. S2 A-D*).

Other possible genes related to pathways regulating KCNQ channels showed no significant change in aged group.

In detail, our findings from the Gene Ontology (GO) enrichment study revealed that aged PVAT had elevated pathways related to inflammatory processes (e.g., GO:0002250, GO:0051249, GO:0002764; mmu05150, mmu05152, mmu04060) (*21*) (Table. S1*). The biological routes and processes involved in the production of

precursor metabolites and energy (e.g., GO:0006091, mmu00190) is down-regulated in the mesenteric PVAT of aged mice (Table. S2*).

A complete overview of these results can be found in:

Yibin Wang, Fatima Yildiz, Andrey Struve, Mario Kassmann, Lajos Markó, May-Britt Köhler, Friedrich C. Luft, Maik Gollasch and Dmitry Tsvetkov. Aging affects K_V7 channels and perivascular-adipose tissue-mediated vascular tone. Front. Physiol., 26 November 2021; 12:749709.

DOI link: https://doi.org/10.3389/fphys.2021.749709.

A copy of this publication is attached.

5. Discussion

Now several results are found regarding the regulation of vascular tone and the vascular dysfunction. First, the findings provide evidence for PVAT down-regulating the vascular tone induced by α1 agonist in mesenteric arteries of young mice, but this kind of PVAT effect is attenuated in aged mice. Second, the study further reveals that QO58-induced relaxation was attenuated by XE991, and it was also attenuated in aged mice. Third, it is verified that K_V7 channels are involved in the regulation of membrane potential and vascular contraction using specific K_V7 channel blocker. Although the research on potassium channels and PVAT has been reflected in many diseases regarding different organs, the relationship and potential mechanism between the two worths further research in terms of hypertension and vascular dysfunction.

5.1 Functions of Perivascular Adipose Tissue in the Vascular System.

PVAT is an adipose tissue existing widely in spinal animals, surrounding the vasculature connecting various organs and tissues. Most part of the PVAT surrounding vessles were a combination of brown and white fat (47), including the mouse mesenteric arteries used here in the experiments. In the study, PVAT was found playing a key role on the anti-contractile effect in mouse mesenteric arteries. This effect is widely discussed through different aspects. On one hand, PVAT may regulate metabolism (*24*) and inflammatory responses (*25*), which in turn has a regulatory effect on vasculitis and vascular remodeling. On the other hand, PVAT affects vascular system reactivity by producing adipokines, cytokines, and vasoactive chemicals, as well as other products (*26*).

5.2 Paracrine Function and Vascular Tone.

Recent studies showed that PVAT mediates arterial tone via paracrine control, thus contributes to vascular dysfunction in many diseases like hypertension, obesity and cardiac disease (*12*). PVAT mediates the blood pressure and vascular biology through SR-A1/VEGF-B axis in obesity (*27*), and it is involved in vascular remodeling via some PVAT-derived factors as adipokines, cytokines (*28*). According to Chang L et al., PVAT is also involved in central circadian systems control of BP rhythmicity (*9*). Increasing production of cytokines and chemokines (i.e. Ang II, IL-1β, IL-6, MCP-1, leptin, TNFα) were detected in PVAT hypertension and obesity, these are factors that involved in the vascular dysfunction (*29-31*).

PVAT is reported to generate substances activating the tyrosine kinase (*32*). Fatty acid (FA)-derived products produced by cytochrome P450 (CYP), lipoxygenase (LOX), and cyclo-oxygenase (COX) are known to modulate cardiovascular function (*33*). Arachidonic acid is a fatty acid that is converted to eicosanoids in vivo (*34*). The COX, LOX, and CYP pathways are the three principal enzyme pathways that produce eicosanoid metabolites. In renal and cardiovascular disorders, the production and metabolism of epoxy fatty acids EETs are impaired (*35, 36*). A vascular relaxation was observed due to the L-type Ca^{2+} channels closing (*34*). CYP2C epoxyeicosatrienoic acids activate large-conductance Ca^{2+}-activated K^+ channels (BK_{Ca}), reported as the cause

for potassium efflux from the smooth muscle cell, which results in membrane hyperpolarization.

It is demonstrated that the role of angiotensin II in hypertension is performed through the production of 12/15-LOX-derived HETEs, which is related to the participation of 12/15-LOX in the control of vascular contraction (*37*).

Prostacyclin (PGI2) is another lipid molecule that belongs to the prostanoid group of eicosanoids that control homeostasis, hemostasis, smooth muscle function, and inflammation. The sequential operations of phospholipase A2, cyclooxygenase (COX), and particular prostaglandin (PG) synthases produce prostanoids from arachidonic acid (*38*). However, the anti-contractile effect of PVAT can be reversed through nitric oxide synthases (NOS) in many animal models (*39-43*).

Former research showed this kind of "adipocyte-derived relaxing factor" (ADRF) works via ATP-dependent potassium channels, moreover, it is independent from cyclooxygenase (COX) or cytochrome P450 (CYP) pathway (*32*), and endothelial prostaglandins or nitric oxide are not involved in this process verified with experiments in lacking of effects of cyclooxygenase or nitric oxide synthase inhibitor on this relaxation factor (*44*). The vasodilation induced by leptin is endothelium dependent (*45*), so the mechanism is far different from the regulation induced by "Perivascular adipose tissue-derived relaxing factors" (PVATRFs). In addition, the measurements of these existing FAs suggested other potential candidates involved in the vascular dysfunction and the regulation of vascular tone.

5.3 K_V7 Channels and anti-contractile effect of PVAT.

Our former study showed the PVAT effect relies on K_V7 channels (*45, 46*), which is also consistent with reports by others. It brought us to further study K_V7 channels. There are five members in the voltage-dependent potassium channel family encoded by the KCNQ genes (*47*). XE991 [10,10-bis(4-pyridinylmethyl)-9(10H)-anthracenone] (*48-50*) and linopirdine [3,3-bis(4-pyridinylmethyl)-1-phenylindolin-2-one] (*51*) are used as the selective blockers of all K_V7 channels. K_V7 channels play important roles in cardiac action potential (*52*) and 'M-current' in neurons (*53*), also the regulation of vascular function as I focused in this study. Additionally, adiponectin is also seen as a potential PVATRF as it can relax mesenteric arteries by opening K_V channels (*54*). There is no significant involvement of the endothelium shown in the ADRF effects in our previous study (*55*). It was reported that 5-HT induces ADRF release from PVAT (*19*). What is more, the PVAT showed anti-contractile properties by activating the VSMC K_V7 channels (*19*). Taken together, it showed us the possibility that K_V7 channels play a significant role in anti-contractile effect of PVAT.

To study the role of K_V7 channels, the following tools were used. Retigabine (*56*) and flupirtine (*57*) were widely used in former research as openers of K_V7 channels.

Pyrazolo[1,5-a]pyrimidin-7(4H)-one compounds (e.g. QO58), are considered as novel KCNQ channel openers, and it is reported that 5-(2,6-Dichloro-5-fluoro-3-pyridinyl)-3-phenyl-2-(trifluoromethyl)-pyrazolo[1,5-a] -pyrimidin-7(4H)-one (QO58) cause the leftward shifts of voltage-dependent activation of K_V7 channels (*21,*

58), QO58 is capable of opening the K_V7 channels (for $K_V7.4$ EC_{50} = 0.6 μM, for $K_V7.3/7.5$ EC_{50} = 5.2 μM) (*17, 21*).

Furthermore, it is demonstrated that PVAT was capable to produce relaxations of mouse mesenteric arteries after pre-contracted by α1 agonist. These effect was inhibited by XE991. In contrast, the anti-contractile effect was attenuated in mouse mesenteric arteries with K_V7 channels openers. Together, these data suggest that XE991 could inhibit anti-contractile effect of PVAT by blocking K_V7 channels in mouse mesenteric arteries.

5.4 Aging and K_V7 Channels.

It has been revealed that aging is the cause of increasing of white blood cells, macrophages and NK cells in PVAT, which induce the perivascular fibrosis a model of spontaneous hypertension (*59*). It is important to note that, aging has different manifestations in many organs, including vascular dysfunction and structural changes (*60*). It can be valued by endothelial elasticity, stiffness, and the superoxide production in PVAT can be promoted by aging (*61*). As aging affects the epigenetic changes in different locations of vessles containing PVAT, smooth muscle cells, endothelium cells and inflammatory cells, these are all related oxidative stress, inflammation and dysfunction in artery tone (*62*). It is previously reported that adiponectin, leptin receptor, PRDM16, PGC-1α, UCP-1 were focused in a PVAT experimental model (*62*). The loss of peroxisome proliferator-activated receptor γ co-activator 1α (PGC-1α) decreases the capacity of brown adipogenic differentiation, it also leads to the elevation of vascular remodeling in aged resident stromal cells (*63*). The process of the transition of adipocyte phenotype is a key part of PVAT modifications led by aging (*63, 64*). Peter Aldiss et al. gave me the new point of view that the brown phenotype of PVAT is an important target for further research, and the released substances are also noteworthy (*65*).

But the aging induced vascular dysfunction could be related to K_V7 channels. In nervous system, aging induced ROS-mediated oxidation of K^+ channels is reported as a strong evidence in a previous study (*66*). The influence of functionally relevant K^+ channels in cochlea and auditory pathways are also reported before (*67*). But for the first time, evidence has been shown K_V7 channels are responsible for the vascular dysfunction due to aging. A significant repolarization caused by K_V7 channel opener was found after the pre-induced depolarization in young mice mesenteric arteries, but no significant repolarization was found in aged mice mesenteric arteries.

5.5 Expression of K_V7 and other Pathways.

The expression of *Kcnq1,3,4,5* mRNA didn't show significant change compairing the mesenteric arteries (-PVAT) of young and old mice, neither did the RNA-seq show additional targets. Our inflammatory transcriptome profile is consistent with the idea that inflammation modulate vascular disorder of aged mouse aorta (*68*), it is however, one of the evidence that low grade inflammation can also cause the vascular

damage in aged mice. Jarkko Soronen et al. have found more details resembles that perivascular fat have similarities regarding insulin resistance patients in the PVAT transcriptional profile, such as downregulated mitochondrial respiratory and lipid metabolic pathways (*69*). It also caters to the report that melatonin treatment can restore the anticontractile properties in aging (*70*). Our study shows same structure in adipose tissue genes participating in fatty acid and triglyceride metabolism (*21*). Thus, other mechanisms like posttranslational modification may have changed in aged mice regarding KCNQ channels that lead to vascular dysfunction.

In conclusion, our study suggested PVAT as novel therapeutic targets in hypertension, and these data suggest that future studies on their roles should consider K_V7 signaling pathways to understand their molecular actions (*21*).

6. Bibliography

1. A. Azarova, D. Irdam, A. Gugushvili, M. Fazekas, G. Scheiring, P. Horvat, D. Stefler, I. Kolesnikova, V. Popov, I. Szelenyi, D. Stuckler, M. Marmot, M. Murphy, M. McKee, M. Bobak, L. King, The effect of rapid privatisation on mortality in mono-industrial towns in post-Soviet Russia: a retrospective cohort study. *Lancet Public Health* **2**, e231-e238 (2017).
2. A. Tran-Dinh, D. Diallo, S. Delbosc, L. M. Varela-Perez, Q. B. Dang, B. Lapergue, E. Burillo, J. B. Michel, A. Levoye, J. L. Martin-Ventura, O. Meilhac, HDL and endothelial protection. *Br J Pharmacol* **169**, 493-511 (2013).
3. A. H. Gradman, Role of angiotensin II type 1 receptor antagonists in the treatment of hypertension in patients aged >or=65 years. *Drugs Aging* **26**, 751-767 (2009).
4. A. McCurley, P. W. Pires, S. B. Bender, M. Aronovitz, M. J. Zhao, D. Metzger, P. Chambon, M. A. Hill, A. M. Dorrance, M. E. Mendelsohn, I. Z. Jaffe, Direct regulation of blood pressure by smooth muscle cell mineralocorticoid receptors. *Nat Med* **18**, 1429-1433 (2012).
5. G. F. Mitchell, Arterial stiffness and hypertension. *Hypertension* **64**, 13-18 (2014).
6. W. Wang, E. T. Lee, R. R. Fabsitz, R. Devereux, L. Best, T. K. Welty, B. V. Howard, A longitudinal study of hypertension risk factors and their relation to cardiovascular disease: the Strong Heart Study. *Hypertension* **47**, 403-409 (2006).
7. M. Writing Group, D. Mozaffarian, E. J. Benjamin, A. S. Go, D. K. Arnett, M. J. Blaha, M. Cushman, S. R. Das, S. de Ferranti, J. P. Despres, H. J. Fullerton, V. J. Howard, M. D. Huffman, C. R. Isasi, M. C. Jimenez, S. E. Judd, B. M. Kissela, J. H. Lichtman, L. D. Lisabeth, S. Liu, R. H. Mackey, D. J. Magid, D. K. McGuire, E. R. Mohler, 3rd, C. S. Moy, P. Muntner, M. E. Mussolino, K. Nasir, R. W. Neumar, G. Nichol, L. Palaniappan, D. K. Pandey, M. J. Reeves, C. J. Rodriguez, W. Rosamond, P. D. Sorlie, J. Stein, A. Towfighi, T. N. Turan, S. S. Virani, D. Woo, R. W. Yeh, M. B. Turner, C. American Heart Association Statistics, S. Stroke Statistics, Heart Disease and Stroke Statistics-2016 Update: A Report From the American Heart Association. *Circulation* **133**, e38-360 (2016).
8. S. Laurent, P. Boutouyrie, The structural factor of hypertension: large and small artery alterations. *Circ Res* **116**, 1007-1021 (2015).
9. L. Chang, W. Xiong, X. Zhao, Y. Fan, Y. Guo, M. Garcia-Barrio, J. Zhang, Z. Jiang, J. D. Lin, Y. E. Chen, Bmal1 in Perivascular Adipose Tissue Regulates Resting-Phase Blood Pressure Through Transcriptional Regulation of Angiotensinogen. *Circulation* **138**, 67-79 (2018).
10. C. G. Barp, D. Bonaventura, J. Assreuy, NO, ROS, RAS, and PVAT: More Than a Soup of Letters. *Front Physiol* **12**, 640021 (2021).
11. J. Y. Tano, J. Schleifenbaum, M. Gollasch, Perivascular adipose tissue, potassium channels, and vascular dysfunction. *Arterioscler Thromb Vasc Biol* **34**, 1827-1830 (2014).

12. M. Gollasch, Adipose-Vascular Coupling and Potential Therapeutics. *Annu Rev Pharmacol Toxicol* **57**, 417-436 (2017).
13. F. Yiannikouris, M. Gupte, K. Putnam, L. Cassis, Adipokines and blood pressure control. *Curr Opin Nephrol Hypertens* **19**, 195-200 (2010).
14. C. Dart, Lipid microdomains and the regulation of ion channel function. *J Physiol* **588**, 3169-3178 (2010).
15. J. Schleifenbaum, C. Kohn, N. Voblova, G. Dubrovska, O. Zavarirskaya, T. Gloe, C. S. Crean, F. C. Luft, Y. Huang, R. Schubert, M. Gollasch, Systemic peripheral artery relaxation by KCNQ channel openers and hydrogen sulfide. *J Hypertens* **28**, 1875-1882 (2010).
16. B. C. Teng, Y. Song, F. Zhang, T. Y. Ma, J. L. Qi, H. L. Zhang, G. Li, K. Wang, Activation of neuronal Kv7/KCNQ/M-channels by the opener QO58-lysine and its anti-nociceptive effects on inflammatory pain in rodents. *Acta Pharmacol Sin* **37**, 1054-1062 (2016).
17. F. Zhang, Y. Mi, J. L. Qi, J. W. Li, M. Si, B. C. Guan, X. N. Du, H. L. An, H. L. Zhang, Modulation of K(v)7 potassium channels by a novel opener pyrazolo[1,5-a]pyrimidin-7(4H)-one compound QO-58. *Br J Pharmacol* **168**, 1030-1042 (2013).
18. J. Qi, F. Zhang, Y. Mi, Y. Fu, W. Xu, D. Zhang, Y. Wu, X. Du, Q. Jia, K. Wang, H. Zhang, Design, synthesis and biological activity of pyrazolo[1,5-a]pyrimidin-7(4H)-ones as novel Kv7/KCNQ potassium channel activators. *Eur J Med Chem* **46**, 934-943 (2011).
19. N. Wang, A. Kuczmanski, G. Dubrovska, M. Gollasch, Palmitic Acid Methyl Ester and Its Relation to Control of Tone of Human Visceral Arteries and Rat Aortas by Perivascular Adipose Tissue. *Front Physiol* **9**, 583 (2018).
20. D. Tsvetkov, J. Y. Tano, M. Kassmann, N. Wang, R. Schubert, M. Gollasch, The Role of DPO-1 and XE991-Sensitive Potassium Channels in Perivascular Adipose Tissue-Mediated Regulation of Vascular Tone. *Front Physiol* **7**, 335 (2016).
21. Y. Wang, F. Yildiz, A. Struve, M. Kassmann, L. Markó, M.-B. Köhler, F. C. Luft, M. Gollasch, D. Tsvetkov, Aging Affects KV7 Channels and Perivascular Adipose Tissue-Mediated Vascular Tone. *Frontiers in Physiology* **12**, (2021).
22. S. Anders, W. Huber, Differential expression analysis for sequence count data. *Genome Biol* **11**, R106 (2010).
23. G. Yu, L. G. Wang, Y. Han, Q. Y. He, clusterProfiler: an R package for comparing biological themes among gene clusters. *OMICS* **16**, 284-287 (2012).
24. L. Chang, L. Villacorta, R. Li, M. Hamblin, W. Xu, C. Dou, J. Zhang, J. Wu, R. Zeng, Y. E. Chen, Loss of perivascular adipose tissue on peroxisome proliferator-activated receptor-gamma deletion in smooth muscle cells impairs intravascular thermoregulation and enhances atherosclerosis. *Circulation* **126**, 1067-1078 (2012).
25. A. S. Greenstein, K. Khavandi, S. B. Withers, K. Sonoyama, O. Clancy, M. Jeziorska, I. Laing, A. P. Yates,

P. W. Pemberton, R. A. Malik, A. M. Heagerty, Local inflammation and hypoxia abolish the protective anticontractile properties of perivascular fat in obese patients. *Circulation* **119**, 1661-1670 (2009).

26. B. C. S. Boa, J. S. Yudkin, V. W. M. van Hinsbergh, E. Bouskela, E. C. Eringa, Exercise effects on perivascular adipose tissue: endocrine and paracrine determinants of vascular function. *Br J Pharmacol* **174**, 3466-3481 (2017).
27. X. Zhu, Y. Wang, L. Zhu, Y. Zhu, K. Zhang, L. Wang, H. Bai, Q. Yang, J. Ben, H. Zhang, X. Li, Y. Xu, Q. Chen, Class A1 scavenger receptor prevents obesity-associated blood pressure elevation through suppressing overproduction of vascular endothelial growth factor B in macrophages. *Cardiovasc Res* **117**, 547-560 (2021).
28. S. Rajsheker, D. Manka, A. L. Blomkalns, T. K. Chatterjee, L. L. Stoll, N. L. Weintraub, Crosstalk between perivascular adipose tissue and blood vessels. *Curr Opin Pharmacol* **10**, 191-196 (2010).
29. Z. B. Zhang, C. C. Ruan, J. R. Lin, L. Xu, X. H. Chen, Y. N. Du, M. X. Fu, L. R. Kong, D. L. Zhu, P. J. Gao, Perivascular Adipose Tissue-Derived PDGF-D Contributes to Aortic Aneurysm Formation During Obesity. *Diabetes* **67**, 1549-1560 (2018).
30. X. Zhu, H. W. Zhang, H. N. Chen, X. J. Deng, Y. X. Tu, A. O. Jackson, J. N. Qing, A. P. Wang, V. Patel, K. Yin, Perivascular adipose tissue dysfunction aggravates adventitial remodeling in obese mini pigs via NLRP3 inflammasome/IL-1 signaling pathway. *Acta Pharmacol Sin* **40**, 46-54 (2019).
31. R. Nosalski, T. J. Guzik, Perivascular adipose tissue inflammation in vascular disease. *Br J Pharmacol* **174**, 3496-3513 (2017).
32. M. Lohn, G. Dubrovska, B. Lauterbach, F. C. Luft, M. Gollasch, A. M. Sharma, Periadventitial fat releases a vascular relaxing factor. *FASEB J* **16**, 1057-1063 (2002).
33. B. Gollasch, G. Wu, I. Dogan, M. Rothe, M. Gollasch, F. C. Luft, Maximal exercise and erythrocyte epoxy fatty acids: a lipidomics study. *Physiol Rep* **7**, e14275 (2019).
34. J. D. Imig, Prospective for cytochrome P450 epoxygenase cardiovascular and renal therapeutics. *Pharmacol Ther* **192**, 1-19 (2018).
35. J. Bellien, R. Joannides, Epoxyeicosatrienoic acid pathway in human health and diseases. *J Cardiovasc Pharmacol* **61**, 188-196 (2013).
36. J. D. Imig, B. D. Hammock, Soluble epoxide hydrolase as a therapeutic target for cardiovascular diseases. *Nat Rev Drug Discov* **8**, 794-805 (2009).
37. Y. Chawengsub, K. M. Gauthier, W. B. Campbell, Role of arachidonic acid lipoxygenase metabolites in the regulation of vascular tone. *Am J Physiol Heart Circ Physiol* **297**, H495-507 (2009).
38. B. H. Majed, R. A. Khalil, Molecular mechanisms regulating the vascular prostacyclin pathways and their adaptation during pregnancy and in the newborn. *Pharmacol Rev* **64**, 540-582 (2012).
39. Y. J. Gao, C. Lu, L. Y. Su, A. M. Sharma, R. M. Lee, Modulation of vascular function by perivascular adipose tissue: the role of endothelium and hydrogen peroxide. *Br J Pharmacol* **151**, 323-331 (2007).
40. F. M. Lynch, S. B. Withers, Z. Yao, M. E. Werner, G. Edwards, A. H. Weston, A. M. Heagerty,

Perivascular adipose tissue-derived adiponectin activates BK(Ca) channels to induce anticontractile responses. *Am J Physiol Heart Circ Physiol* **304**, H786-795 (2013).

41. C. E. Bussey, S. B. Withers, R. G. Aldous, G. Edwards, A. M. Heagerty, Obesity-Related Perivascular Adipose Tissue Damage Is Reversed by Sustained Weight Loss in the Rat. *Arterioscler Thromb Vasc Biol* **36**, 1377-1385 (2016).
42. K. E. Zaborska, M. Wareing, G. Edwards, C. Austin, Loss of anti-contractile effect of perivascular adipose tissue in offspring of obese rats. *Int J Obes (Lond)* **40**, 1205-1214 (2016).
43. R. Aghamohammadzadeh, R. D. Unwin, A. S. Greenstein, A. M. Heagerty, Effects of Obesity on Perivascular Adipose Tissue Vasorelaxant Function: Nitric Oxide, Inflammation and Elevated Systemic Blood Pressure. *J Vasc Res* **52**, 299-305 (2015).
44. Y. J. Gao, Z. H. Zeng, K. Teoh, A. M. Sharma, L. Abouzahr, I. Cybulsky, A. Lamy, L. Semelhago, R. M. Lee, Perivascular adipose tissue modulates vascular function in the human internal thoracic artery. *J Thorac Cardiovasc Surg* **130**, 1130-1136 (2005).
45. G. Lembo, C. Vecchione, L. Fratta, G. Marino, V. Trimarco, G. d'Amati, B. Trimarco, Leptin induces direct vasodilation through distinct endothelial mechanisms. *Diabetes* **49**, 293-297 (2000).
46. S. Verlohren, G. Dubrovska, S. Y. Tsang, K. Essin, F. C. Luft, Y. Huang, M. Gollasch, Visceral periadventitial adipose tissue regulates arterial tone of mesenteric arteries. *Hypertension* **44**, 271-276 (2004).
47. J. B. Stott, T. A. Jepps, I. A. Greenwood, K(V)7 potassium channels: a new therapeutic target in smooth muscle disorders. *Drug Discov Today* **19**, 413-424 (2014).
48. H. S. Wang, B. S. Brown, D. McKinnon, I. S. Cohen, Molecular basis for differential sensitivity of KCNQ and I(Ks) channels to the cognitive enhancer XE991. *Mol Pharmacol* **57**, 1218-1223 (2000).
49. H. S. Jensen, K. Callo, T. Jespersen, B. S. Jensen, S. P. Olesen, The KCNQ5 potassium channel from mouse: a broadly expressed M-current like potassium channel modulated by zinc, pH, and volume changes. *Brain Res Mol Brain Res* **139**, 52-62 (2005).
50. S. Y. Yeung, V. Pucovsky, J. D. Moffatt, L. Saldanha, M. Schwake, S. Ohya, I. A. Greenwood, Molecular expression and pharmacological identification of a role for K(v)7 channels in murine vascular reactivity. *Br J Pharmacol* **151**, 758-770 (2007).
51. D. S. Dupuis, R. L. Schroder, T. Jespersen, J. K. Christensen, P. Christophersen, B. S. Jensen, S. P. Olesen, Activation of KCNQ5 channels stably expressed in HEK293 cells by BMS-204352. *Eur J Pharmacol* **437**, 129-137 (2002).
52. J. Barhanin, F. Lesage, E. Guillemare, M. Fink, M. Lazdunski, G. Romey, K(V)LQT1 and lsK (minK) proteins associate to form the I(Ks) cardiac potassium current. *Nature* **384**, 78-80 (1996).
53. D. A. Brown, P. R. Adams, Muscarinic suppression of a novel voltage-sensitive K^+ current in a vertebrate neurone. *Nature* **283**, 673-676 (1980).
54. G. Fesus, G. Dubrovska, K. Gorzelniak, R. Kluge, Y. Huang, F. C. Luft, M. Gollasch, Adiponectin is a

novel humoral vasodilator. *Cardiovasc Res* **75**, 719-727 (2007).

55. M. A. Oriowo, Perivascular adipose tissue, vascular reactivity and hypertension. *Med Princ Pract* **24 Suppl 1**, 29-37 (2015).
56. V. Vellecco, A. Martelli, I. S. Bibli, M. Vallifuoco, O. L. Manzo, E. Panza, V. Citi, V. Calderone, G. de Dominicis, C. Cozzolino, E. M. Basso, M. Mariniello, I. Fleming, A. Mancini, M. Bucci, G. Cirino, Anomalous Kv 7 channel activity in human malignant hyperthermia syndrome unmasks a key role for H2 S and persulfidation in skeletal muscle. *Br J Pharmacol* **177**, 810-823 (2020).
57. X. Zhou, J. Wei, M. Song, K. Francis, S. P. Yu, Novel role of KCNQ2/3 channels in regulating neuronal cell viability. *Cell Death Differ* **18**, 493-505 (2011).
58. C. Tabula Muris, A single-cell transcriptomic atlas characterizes ageing tissues in the mouse. *Nature* **583**, 590-595 (2020).
59. R. Nosalski, T. Mikolajczyk, M. Siedlinski, B. Saju, J. Koziol, P. Maffia, T. J. Guzik, Nox1/4 inhibition exacerbates age dependent perivascular inflammation and fibrosis in a model of spontaneous hypertension. *Pharmacol Res* **161**, 105235 (2020).
60. M. R. Meyer, N. C. Fredette, C. Daniel, G. Sharma, K. Amann, J. B. Arterburn, M. Barton, E. R. Prossnitz, Obligatory role for GPER in cardiovascular aging and disease. *Sci Signal* **9**, ra105 (2016).
61. B. S. Fleenor, J. S. Eng, A. L. Sindler, B. T. Pham, J. D. Kloor, D. R. Seals, Superoxide signaling in perivascular adipose tissue promotes age-related artery stiffness. *Aging Cell* **13**, 576-578 (2014).
62. M. Queiroz, C. M. Sena, Perivascular adipose tissue in age-related vascular disease. *Ageing Res Rev* **59**, 101040 (2020).
63. X. X. Pan, C. C. Ruan, X. Y. Liu, L. R. Kong, Y. Ma, Q. H. Wu, H. Q. Li, Y. J. Sun, A. Q. Chen, Q. Zhao, F. Wu, X. J. Wang, J. G. Wang, D. L. Zhu, P. J. Gao, Perivascular adipose tissue-derived stromal cells contribute to vascular remodeling during aging. *Aging Cell* **18**, e12969 (2019).
64. L. R. Kong, Y. P. Zhou, D. R. Chen, C. C. Ruan, P. J. Gao, Decrease of Perivascular Adipose Tissue Browning Is Associated With Vascular Dysfunction in Spontaneous Hypertensive Rats During Aging. *Front Physiol* **9**, 400 (2018).
65. P. Aldiss, G. Davies, R. Woods, H. Budge, H. S. Sacks, M. E. Symonds, 'Browning' the cardiac and peri-vascular adipose tissues to modulate cardiovascular risk. *Int J Cardiol* **228**, 265-274 (2017).
66. S. Q. Cai, F. Sesti, Oxidation of a potassium channel causes progressive sensory function loss during aging. *Nat Neurosci* **12**, 611-617 (2009).
67. B. Peixoto Pinheiro, B. Vona, H. Lowenheim, L. Ruttiger, M. Knipper, Y. Adel, Age-related hearing loss pertaining to potassium ion channels in the cochlea and auditory pathway. *Pflugers Arch* **473**, 823-840 (2021).
68. P. Gao, P. Gao, M. Choi, K. Chegireddy, O. J. Slivano, J. Zhao, W. Zhang, X. Long, Transcriptome analysis of mouse aortae reveals multiple novel pathways regulated by aging. *Aging (Albany NY)* **12**, 15603-15623 (2020).

69. J. Soronen, P. P. Laurila, J. Naukkarinen, I. Surakka, S. Ripatti, M. Jauhiainen, V. M. Olkkonen, H. Yki-Jarvinen, Adipose tissue gene expression analysis reveals changes in inflammatory, mitochondrial respiratory and lipid metabolic pathways in obese insulin-resistant subjects. *BMC Med Genomics* **5**, 9 (2012).

70. C. Agabiti-Rosei, G. Favero, C. De Ciuceis, C. Rossini, E. Porteri, L. F. Rodella, L. Franceschetti, A. Maria Sarkar, E. Agabiti-Rosei, D. Rizzoni, R. Rezzani, Effect of long-term treatment with melatonin on vascular markers of oxidative stress/inflammation and on the anticontractile activity of perivascular fat in aging mice. *Hypertens Res* **40**, 41-50 (2017).

7. Affidavit

I, Yibin Wang, by personally signing this document in lieu of an oath, hereby affirm that I prepared the submitted dissertation on the topic Roles of Perivascular Adipose Tissue and K_V7 Voltage-dependent Potassium Channels in Vascular Tone (Rollen des perivaskulären Fettgewebes und der spannungsabhängigen K_V7-Kaliumkanäle im Gefäßtonus). I wrote this dissertation independently and without assistance from third parties, and that I used no other sources and aids than those stated.
All parts which are based on the publications or presentations of other authors, either in letter or in spirit, are specified as such in accordance with the citing guidelines. The sections on methodology (in particular regarding practical work, laboratory regulations, statistical processing) and results (in particular regarding figures, charts and tables) are exclusively my responsibility.

Furthermore, I declare that I have correctly marked all of the data, the analyses, and the conclusions generated from data obtained in collaboration with other persons, and that I have correctly marked my own contribution and the contributions of other persons (cf. declaration of contribution). I have correctly marked all texts or parts of texts that were generated in collaboration with other persons.

My contributions to any publications to this dissertation correspond to those stated in the below joint declaration made together with the supervisor. All publications created within the scope of the dissertation comply with the guidelines of the ICMJE (International Committee of Medical Journal Editors; www.icmje.org) on authorship. In addition, I declare that I shall comply with the regulations of Charité – Universitätsmedizin Berlin on ensuring good scientific practice.

I declare that I have not yet submitted this dissertation in identical or similar form to another Faculty.

The significance of this statutory declaration and the consequences of a false statutory declaration under criminal law (Sections 156, 161 of the German Criminal Code) are known to me."

Date

Signature

7.1 Declaration of any eventual publications

Yibin Wang have the following share in the publications below:

Yibin Wang, Fatima Yildiz, Andrey Struve, Mario Kassmann, Lajos Markó, May-Britt Köhler, Friedrich C. Luft, Maik Gollasch and Dmitry Tsvetkov. Aging affects K_V7 channels and perivascular-adipose tissue-mediated vascular tone. Front. Physiol., 26 November 2021; 12:749709.

DOI link: https://doi.org/10.3389/fphys.2021.749709. Impact Factor (2020/2021): 4.566

Contribution:

Yibin Wang, Fatima Yildiz, Andrey Struve, Mario Kassmann, Friedrich C. Luft, Maik Gollasch and Dmitry Tsvetkov were responsible for data collection, and interpretation. Yibin Wang did preparation of vessels and collected data using wire-myography and sharp electrodes membrane potential setup. Yibin Wang drawed Figure 1, Figure 3, panel E and F of Figure 4, Figure S1 basing on these data. Yibin Wang also extracted mRNA and performed reverse transcription and quantitative real-time PCR, as well as the data analysis, Yibin Wang drawed Figure S2 basing on these data. Yibin Wang and Dr. Dmitry Tsvetkov prepared the first draft of the manuscript. Prof. Dr. med. Dr. rer. nat. Maik Gollasch, Prof. Dr. Friedrich C. Luft, Fatima Yildiz, Andrey Struve, Mario Kassmann, Lajos Markó, May-Britt Köhler contributed to the completion of the manuscript.

Signature, date and stamp of the supervising university teacher

Prof. Dr. med. Dr. rer. nat. Maik Gollasch

Signature of doctoral student

Yibin Wang

8. Selected Publications

Yibin Wang, Fatima Yildiz, Andrey Struve, Mario Kassmann, Lajos Markó, May-Britt Köhler, Friedrich C. Luft, Maik Gollasch and Dmitry Tsvetkov. Aging affects K_V7 channels and perivascular-adipose tissue-mediated vascular tone. Front. Physiol., 26 November 2021; 12:749709. DOI link: https://doi.org/10.3389/fphys.2021.749709.

Journal Data Filtered By: **Selected JCR Year: 2020** Selected Editions: SCIE,SSCI
Selected Categories: **"PHYSIOLOGY"** Selected Category Scheme: WoS
Gesamtanzahl: 81 Journale

Rank	Full Journal Title	Total Cites	Journal Impact Factor	Eigenfactor Score
1	PHYSIOLOGICAL REVIEWS	35,633	37.312	0.023380
2	Annual Review of Physiology	11,515	19.318	0.009940
3	JOURNAL OF PINEAL RESEARCH	12,492	13.007	0.008170
4	Comprehensive Physiology	6,720	9.090	0.008250
5	PHYSIOLOGY	4,651	8.831	0.005060
6	International Journal of Behavioral Nutrition and Physical Activity	14,522	6.457	0.018810
7	JOURNAL OF CELLULAR PHYSIOLOGY	39,997	6.384	0.041830
8	Acta Physiologica	6,448	6.311	0.006870
9	EXERCISE AND SPORT SCIENCES REVIEWS	4,053	6.230	0.002770
10	Reviews of Physiology Biochemistry and Pharmacology	865	5.545	0.000390
11	AMERICAN JOURNAL OF PHYSIOLOGY-LUNG CELLULAR AND MOLECULAR PHYSIOLOGY	16,880	5.464	0.014100
12	JOURNAL OF PHYSIOLOGY-LONDON	58,028	5.182	0.034600
13	AMERICAN JOURNAL OF PHYSIOLOGY-HEART AND CIRCULATORY PHYSIOLOGY	30,771	4.733	0.016970
14	Frontiers in Physiology	35,008	4.566	0.063610
15	AMERICAN JOURNAL OF PHYSIOLOGY-ENDOCRINOLOGY AND METABOLISM	22,017	4.310	0.011400
16	AMERICAN JOURNAL OF PHYSIOLOGY-CELL PHYSIOLOGY	18,210	4.249	0.009500
17	JOURNAL OF PHYSIOLOGY AND BIOCHEMISTRY	2,365	4.158	0.002390

frontiers in Physiology

ORIGINAL RESEARCH
published: 26 November 2021
doi: 10.3389/fphys.2021.749709

Aging Affects K_V7 Channels and Perivascular Adipose Tissue-Mediated Vascular Tone

Yibin Wang[1], Fatima Yildiz[2], Andrey Struve[3], Mario Kassmann[1,4], Lajos Markó[1], May-Britt Köhler[1], Friedrich C. Luft[1], Maik Gollasch[1,4] and Dmitry Tsvetkov[1,4]**

[1]Charité Medical Faculty, Experimental and Clinical Research Center (ECRC), Max Delbrück Center for Molecular Medicine (MDC), Berlin, Germany, [2]Faculty of Medicine, Istanbul Medeniyet University, Istanbul, Turkey, [3]Department of Ear, Throat and Nose Diseases, I.M. Sechenov First Moscow State Medical University, Moscow, Russia, [4]Department of Internal Medicine and Geriatrics, University Medicine Greifswald, Greifswald, Germany

Aging is an independent risk factor for hypertension, cardiovascular morbidity, and mortality. However, detailed mechanisms linking aging to cardiovascular disease are unclear. We studied the aging effects on the role of perivascular adipose tissue and downstream vasoconstriction targets, voltage-dependent K_V7 channels, and their pharmacological modulators (flupirtine, retigabine, QO58, and QO58-lysine) in a murine model. We assessed vascular function of young and old mesenteric arteries *in vitro* using wire myography and membrane potential measurements with sharp electrodes. We also performed bulk RNA sequencing and quantitative reverse transcription-polymerase chain reaction tests in mesenteric arteries and perivascular adipose tissue to elucidate molecular underpinnings of age-related phenotypes. Results revealed impaired perivascular adipose tissue-mediated control of vascular tone particularly *via* $K_V7.3–5$ channels with increased age through metabolic and inflammatory processes and release of perivascular adipose tissue-derived relaxation factors. Moreover, QO58 was identified as novel pharmacological vasodilator to activate XE991-sensitive KCNQ channels in old mesenteric arteries. Our data suggest that targeting inflammation and metabolism in perivascular adipose tissue could represent novel approaches to restore vascular function during aging. Furthermore, $K_V7.3–5$ channels represent a promising target in cardiovascular aging.

Keywords: aging, K_V7 channels, perivascular adipose tissue, transcriptome, RNA sequencing

OPEN ACCESS

Edited by:
Nuria Villalba, University of South Florida, United States

Reviewed by:
George C. Wellman, University of Vermont, United States
William F. Jackson, Michigan State University, United States

****Correspondence:***
Dmitry Tsvetkov
dmitry.tsvetkov@charite.de
Maik Gollasch
maik.gollasch@charite.de

Specialty section:
This article was submitted to Vascular Physiology, a section of the journal Frontiers in Physiology

Received: *29 July 2021*
Accepted: *26 October 2021*
Published: *26 November 2021*

Citation:
Wang Y, Yildiz F, Struve A, Kassmann M, Markó L, Köhler M-B, Luft FC, Gollasch M and Tsvetkov D (2021) Aging Affects K_V7 Channels and Perivascular Adipose Tissue-Mediated Vascular Tone. Front. Physiol. 12:749709. doi: 10.3389/fphys.2021.749709

INTRODUCTION

Hypertension is the leading risk factor of death worldwide, especially for persons aged 50–74 years and 75 years and older (Collaborators, 2020). Human life expectancy is increasing steadily, which will further amplify age-related effects (Vollset et al., 2020). Rigorous research is necessary to address these challenges. Despite remarkable progress in understanding molecular biology of aging, detailed mechanisms linking aging to cardiovascular disease are still unclear (North and Sinclair, 2012). Mice are a utilitarian model to investigate age-related effects (Dupont et al., 2016). Our past studies have shed light on the regulation of vasculature tone by perivascular adipose tissue (PVAT; Gollasch, 2017). Fatty tissue surrounding blood vessels is

now recognized as an integral endocrine/paracrine organ. In addition to the endothelium, PVAT releases vasoactive compounds to cause relaxation of blood vessels known as the anticontractile effect of PVAT (Lohn et al., 2002). PVAT relaxation factors (PVATRFs) have been proposed and such factors could be pivotal in aging. Our earlier work suggests that PVAT paracrine effects are caused by opening of potassium (K^+) channels in vascular smooth muscle cells (Verlohren et al., 2004). The KCNQ-type, K_V7 channels represent the most likely candidates as largely supported by studies with XE991, a highly effective blocker of these channels (Schleifenbaum et al., 2010; Tsvetkov et al., 2017). In fact, the K_V7 family represents a new target for hypertension treatment (Schleifenbaum et al., 2010; Jepps et al., 2011; Mani et al., 2016). K_V7 channel function determines sensitivity to key regulators of coronary tone in diabetes, which expands therapeutic potential even further (Morales-Cano et al., 2015; Barrese et al., 2018). However, toxicity issues of currently available K_V7 channel modulators, such as retigabine and flupirtine, have hampered drug development directed at this target (FDA, 2013; European Medicines Agency, 2018). Pyrazolo[1,5-a]pyrimidin-7(4H)-one compounds (e.g., QO58) have been identified as novel KCNQ channel openers, which can cause remarkable leftward shifts of voltage-dependent activation of K_V7 channels (Jia et al., 2011). Newly emerging RNA sequencing technologies coupled with established techniques could enable researching these new compounds (Tabula Muris, 2020). We hypothesize that age could attenuate the effects of PVAT as mediated by K_V7 channels. We employed the established flupirtine and retigabine, as well as novel compounds (QO58 and QO58-lysine) as K_V7 channel activators in isolated mesenteric arteries from young and old mice.

MATERIALS AND METHODS

Mouse Model

We used young (11–18 weeks old), 12-month old (50–54 weeks), 16-month old (66–69 weeks), and 24-month old (105–106 weeks) male wild-type mice C57BL/6 N. Animal care followed American Physiological Society guidelines, and local authorities (Landesamt für Gesundheit und Soziales Berlin, LAGeSo) approved all protocols. Mice were housed in individually ventilated cages under standardized conditions with an artificial 12-h dark–light cycle with free access to water and food. Animals were randomly assigned to the experimental procedures in accordance with the German legislation on protection of animals.

Wire Myography

Mesenteric arteries were isolated after sacrifice with isoflurane anesthesia, as previously described (Tsvetkov et al., 2017). Then, blood vessels were quickly transferred to cold (4°C), oxygenated (95% O_2/5% CO_2) physiological salt solution (PSS) containing (in mmol/L) 119 NaCl, 4.7 KCl, 1.2 KH_2PO_4, 25 $NaHCO_3$, 1.2 Mg_2SO_4, 11.1 glucose, and 1.6 $CaCl_2$. We dissected the vessels into 2 mm rings whereby perivascular fat and connective tissue were either intact [(+) PVAT] or removed [(−) PVAT rings]. Each ring was placed between two stainless steel wires (diameter 0.0394 mm) in a 5-ml organ bath of a Mulvany Small Vessel Myograph (DMT 610 M; Danish Myo Technology, Denmark). The organ bath was filled with PSS. Continuously oxygenated bath solution with a gas mixture of 95% O_2 and 5% CO_2 was kept at 37°C (pH 7.4). To obtain the passive diameter of the vessel at 100 mm Hg, a DMT normalization procedure was performed. The mesenteric artery rings were placed under a tension equivalent to that generated at 0.9 times the diameter of the vessel at 100 mm Hg by stepwise distending the vessel using LabChart DMT Normalization module. The software Chart5 (AD Instruments Ltd. Spechbach, Germany) was used for data acquisition and display. After 60-min incubation, arteries were precontracted either with isotonic external 60 mm KCl or 1–3 µm phenylephrine (PE), or methoxamine (ME) until a stable resting tension was acquired. The composition of 60 mM KCl (in mmol/L) was 63.7 NaCl, 60 KCl, 1.2 KH_2PO_4, 25 $NaHCO_3$, 1.2 Mg_2SO_4, 11.1 glucose, and 1.6 $CaCl_2$. Drugs were added to the bath solution if not indicated otherwise. Tension is expressed as a percentage of the steady-state tension (100%) obtained with isotonic external 60 mm KCl or agonist (e.g., PE and ME).

Membrane Potential Recordings

Intracellular recordings of membrane potential in smooth muscle cells of intact mesenteric arteries were made using microelectrodes pulled from aluminosilicate glass and filled with 3 M KCl as previously described (Zavaritskaya et al., 2020). An amplifier (DUO 773, World Precision Instruments) was used to record the membrane potential. We used a micromanipulator (UMP, Sensapex) to make impalements from the vessel's adventitial side. The following criteria for acceptance of membrane potential recordings were used: (1) an abrupt change in membrane potential upon cell penetration; (2) a constant electrode resistance when compared before, during, and after the measurement; (3) a stable reading of the membrane potential lasting longer than 1 min; and (4) no change in the baseline when the electrode was removed.

Histology

Formalin-fixed, paraffin-embedded, 4-µm-thick sections were hematoxylin- and eosin-stained using standard protocols. Sections were scanned using the Slide Scanner Pannoramic MIDI (3DHistech Ltd., Hungary) with the objective plan-apochromat 20x (ZEISS, Germany). Forty randomly chosen fat cells were measured and analyzed using CaseViewer (3DHistech Ltd., Hungary) software, and mean perimeter and area were calculated. Immunohistochemical staining of Ly-6B.2-positive cells was performed on 4-µm-thick formalin-fixed, paraffin-embedded sections. Antigen retrieval was performed by incubating sections for 10 min at 37°C in a trypsin solution (Sigma). After cooling down, non-specific binding sites were blocked with 10% normal donkey serum for 30 min following incubation with rat anti-mouse Ly-6B.2

monoclonal antibody (MCA771G, AbD Serotec, clone 7/4, dilution: 1:300) overnight at 4°C in a humid chamber. For fluorescence visualization of bound primary antibody, sections were further incubated with Cy3-conjugated secondary antibody for 1 h in a humid chamber at room temperature. Specimens were analyzed using a Zeiss Axioplan-2 imaging microscope with AxioVision 4.8 software (Zeiss, Jena, Germany). The investigator had no knowledge of the treatment group assignment. Ly-6B.2-positive cells were counted through the whole section using 400X magnification; mean of two sections are presented.

Quantitative Real-Time PCR

Total RNA was isolated from young, 12-, 16-, and 24-month-old mice mesenteric arteries (first branches) by using the RNeasy RNA isolation kit (Qiagen, Germantown, MD) according to the manufacturer's instruction. Isolated RNA concentration was measured, and RNA quality was tested by NanoDrop-1000 spectrophotometer (Thermo Fisher Scientific, Vernon Hills, IL). Two micrograms of RNA was used for cDNA transcription (Applied Biosystems, Foster City, CA). Experiments were run on an Applied Biosystems 7500 Fast Real-Time PCR System (Life Technologies Corporation, Carlsbad, CA, United States). Primers were designed using Primer 3 software on different exons to exclude any DNA contamination. Specificity of amplified products was validated *in silico* (blast) and empirically with gel electrophoresis and analysis of melt curves. Primers were synthesized by BioTez (Berlin, Germany); the sequences are provided below. The cycling conditions were the following: initial activation at 95°C for 10 min, followed by 40 cycles at 95°C for 15 s and 60°C for 1 min. Samples and negative controls were run in parallel. Quantitative analysis of target mRNA expression was performed with quantitative real-time PCR using the relative standard curve method. The expression level of the target genes was normalized by the expression of *18 s*. Under our experimental conditions, expression of *18 s* as a reference gene did not differ between young and old mice tissues. The fold change in gene expression between young and old mice was calculated using $2^{\Delta\Delta Ct}$ method. The following primers were used:

18 s: F: 5′-ACATCCAAGGAAGGCAGCAG-3′;
R: 5′-TTTTCGTCACTACCTCCCCG-3′.
Kcnq1: F: 5′-AGCAGTATGCCGCTCTGG-3′;
R: 5′-AGATGCCCACGTACTTGCTG-3′.
Kcnq3: F: 5′-CAGTATTCGGCCGGACATCT-3′;
R: 5′-GAGACTGCTGGGATGGGTAG-3′.
Kcnq4: F: 5′-CACTTTGAGAAGCGCAGGAT-3′;
R: 5′-CCAGGTGGCTGTCAAATAGG-3′.
Kcnq5: F: 5′-CCTCACTACGGCTCAAGAGT-3′;
R: 5′-TTAAGTGGTGGGGTGAGGTC-3′.

RNA Sequencing

Following Agilent 2100 bioanalyzer quality control, RNA-seq was performed using Illumina Genome Analyzer Novaseq 6000 platform. NEB Next® Ultra™ RNA Library Prep Kit was used for library preparation. Sequence quality estimations, GC content, nucleotide distribution, and read duplication levels were determined for the samples using fastp-0.12.2 software. The reads were mapped to the reference mouse genome (ensembl_mus_musculus_grcm38_p6_gca_000001635_8). HISAT2 was selected to map the filtered sequenced reads to the reference genome. The uniquely mapped read data output was processed using custom scripts in R software (version 3.5.1) and then normalized using the FeatureCounts package v1.5.0-p3 version. Differential expression analysis was performed using the DESeq2 R package version v1.20.0 (Anders and Huber, 2010). We used clusterProfiler for enrichment analysis, including GO Enrichment, DO Enrichment, Kyoto Encyclopedia of Genes and Genomes (KEGG), and Reactome database Enrichment (Yu et al., 2012). Heat map was generated based on fragments per kilobase per million mapped fragments values using Morpheus software.[1]

Materials

All salts and other chemicals were purchased from Sigma-Aldrich (Germany) or Merck (Germany). Using DMSO or PSS, drugs were freshly dissolved on the day of each experiment accordingly to the material sheet. Maximal DMSO concentration after application did not exceed 0.5%. Following concentration of drugs was used: phenylephrine (Sigma-Aldrich) and methoxamine (Sigma-Aldrich) ranged from 0.01 to 100 µm; retigabine (Valeant Research North America), flupirtine (Tocris), QO58 (Tocris), QO58-lysine from 0.01 to 30 µm; 3 µm XE991 (Tocris).

Statistics

Data present mean ± SEM. We calculated EC_{50} values using a Hill equation: $T = (B_0 - Be)/(1 + ([D]/EC_{50})^n) + Be$, where T is the tension in response to the drug (D); Be is the maximum response induced by the drug; B_0, is a constant; EC_{50} is the concentration of the drug that elicits a half-maximal response.

For curve fittings using non-linear regression, GraphPad 8.0.1 (Software, La Jolla California United States) software was used. Statistical significance was determined by Mann–Whitney test or nonparametric ANOVA (Kruskal-Wallis test). Extra sum-of-squares F test was performed for comparison of concentration-response curves. Values of $p < 0.05$ were considered statistically significant. n represents the number of arteries; N represents the number of mice tested. Figures were made using Coreldraw Graphics Suite 2020 (Ottawa, Canada).

RESULTS

Aging Impairs PVAT-Mediated Control of Vascular Tone

First, we examined the role of aging in the anticontractile effects of PVAT. Isolated mesenteric arteries were contracted by alpha1 adrenoceptor (alpha1-AR) stimulation with methoxamine (ME).

[1]https://software.broadinstitute.org/morpheus

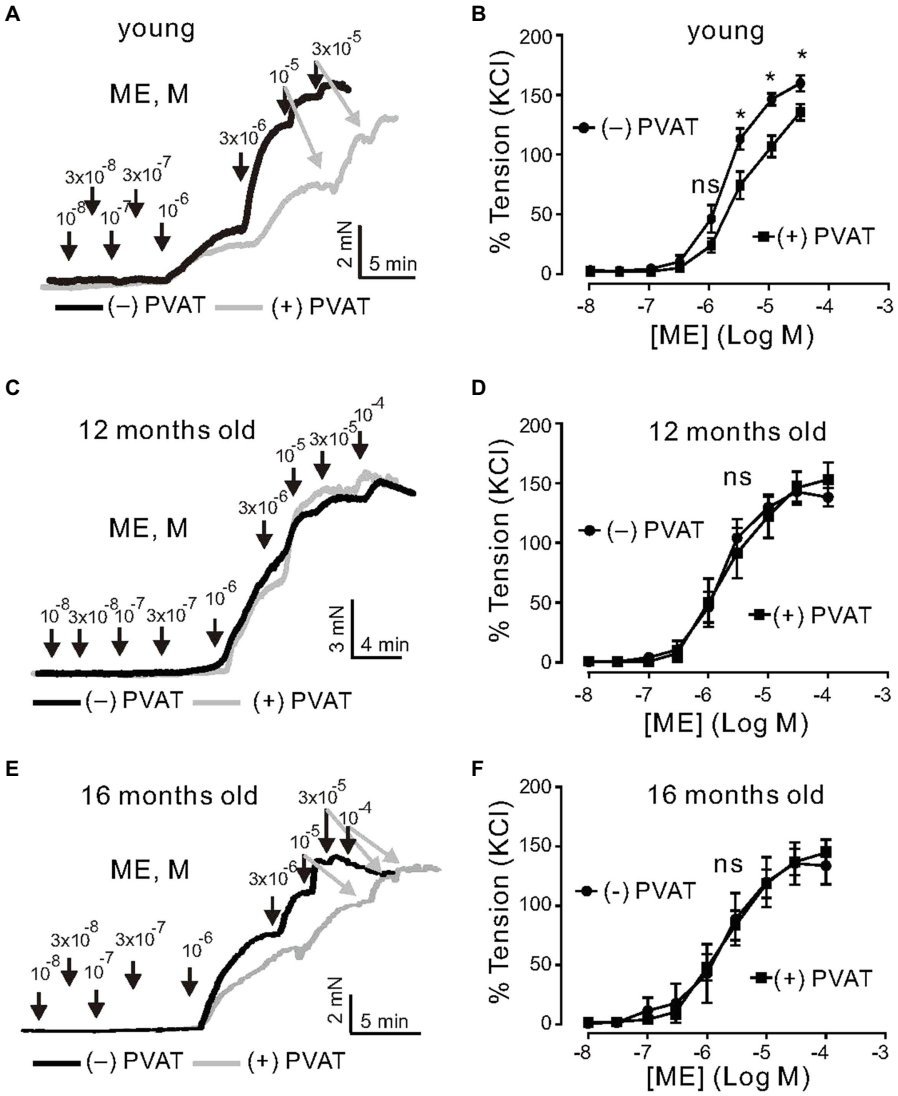

FIGURE 1 | Effects of aging on regulation of arterial tone by a1-agonists Methoxamine (ME) and perivascular adipose tissue (PVAT). **(A)** Original traces showing a1-agonist-induced contractions in (–) PVAT and (+) PVAT mesenteric artery rings isolated from young mice. **(B)** Concentration-response relationships for a1-agonist-induced contractions in (–) PVAT ($n = 10$, $N = 5$) or (+) PVAT ($n = 10$, $N = 4$) mesenteric arteries from young animals. **(C)** Original traces showing aging effects on a1-agonist-induced contractions in (–) PVAT and (+) PVAT mesenteric artery rings isolated from 12-month-old mice. **(D)** Concentration-response relationships for a1-agonist-induced contractions of (+) PVAT ($n = 6$, $N = 2$) and (–) PVAT ($n = 9$, $N = 2$) artery rings isolated from 12-month-old mice. **(E)** Original traces showing aging effects on a1-agonist-induced contractions in (–) PVAT and (+) PVAT mesenteric artery rings isolated from 16-month-old mice. **(F)** Cumulative concentration-response relationships to a1-agonist in (–) PVAT ($n = 7$, $N = 3$) and (+) PVAT ($n = 9$, $N = 3$) mesenteric arteries in 16-month-old mice. *$p < 0.05$. Two-way ANOVA followed by Bonferroni *post hoc* test. Data are mean and SEM.

To test whether or not PVAT regulation on the arterial tone is impaired with aging, we performed a series of experiments using arteries from young (3 months old), 12-, and 16-month-old mice (**Figure 1**). Arteries were prepared either with (+) PVAT or without (–) PVAT. Mesenteric artery rings of young mice displayed strong anticontractile effects of PVAT, namely, the concentration-response curve for vasocontractions of (+) PVAT rings by ME was shifted to the right, compared to (–) PVAT rings (**Figures 1A,B**). In contrast, (–) PVAT artery rings from 1-year-old mice displayed contractions in response to alpha1-AR agonist similar to (+) PVAT rings (**Figures 1C,D**). To substantiate the results, we performed similar experiments using artery rings isolated from 16-month-old mice. Alpha1-AR agonist-induced contractions were similar between (–) PVAT rings and (+) PVAT rings (**Figures 1E,F**). Together, the results suggest that the anticontractile effects of PVAT are impaired in aging.

K_V7 Channel Function in PVAT Is Affected by Age

Next, we assessed the role of K_V7 channels during aging. K_V7 channels were activated by flupirtine and retigabine, which are

considered as potent KCNQ3-5 activators in vascular smooth muscle (Tsvetkov et al., 2017). Flupirtine produced concentration-dependent relaxations; however, the effects were reduced by increased age. For instance, in arterial rings from 12- and 24-month-old mice, the effects were clearly age-dependent (**Figures 2A,B**). The 95% CI for EC_{50} of young, 12-, and 24-month-old mice rings were 0.6–0.8 µm, 1.8–4.8 µm, and 12.4–43.3 µm, respectively. Retigabine caused similar effects (**Figures 2C,D**).

We tested two novel K_V7 channel activators, namely, QO58 and QO58-lysine. QO58 produced concentration-dependent relaxations. The effects were abolished by 3 µM XE991 (pan K_V7 channel blocker) at low QO58 concentrations (<1 µm; **Figures 3A,B**). In contrast, XE991 was unable to inhibit relaxations induced by QO58-lysine (**Figures 3C,D**). The data suggest that OQ58 but not QO58-lysine is capable of producing arterial relaxations through activation of XE991 sensitive KCNQ channels. Similar to flupirtine and retigabine, aging attenuated QO58-induced relaxations (**Figure 3E**). Aged mice mesenteric arteries displayed normal resting membrane potential (**Supplementary Figures S1A–C**). However, 3 µm QO58 caused hyperpolarization of the membrane potential only in young mice; this hyperpolarization was reversed by 3 µm XE991 in young (**Supplementary Figures S1D,E**) but not in old arteries (**Supplementary Figures S1F,G**). Simultaneously measured tension confirmed previously obtained results whereas XE991-induced depolarization led to contraction of young but not old vessels (**Supplementary Figures S1D,F,H; Figures 3A,B**). Thus, our data indicate that KCNQ channel function is impaired in aging.

Then, we determined whether or not the effects of flupirtine, retigabine, QO58, and QO58-lysine rely on K^+ channel activation. Raising external [K^+] to 60 mm would be expected to diminish the effects of any K^+ channel opener by substantially reducing the difference between the potassium equilibrium potential and membrane potential. In these conditions, contractions are primarily caused by Ca^{2+} influx through L-type $Ca_V1.2$ channels resistant to K^+ channel openers (Essin et al., 2007). We found that flupirtine, retigabine, QO58, and QO58-lysine produced moderate relaxation only at relatively high (≥30 µm) concentrations (**Figures 4A–D**). Vehicle application produced no relaxations (**Figures 4E,F**). Therefore, all four KCNQ channel activators may have off-target effects either on downstream targets regulating Ca^{2+} channels or L-type $Ca_V1.2$ channels itself, only at higher concentrations (≥ 30 µm).

RNA Sequencing

To examine age-related changes in mRNA expression in mesenteric arteries and PVAT, we performed targeted and bulk

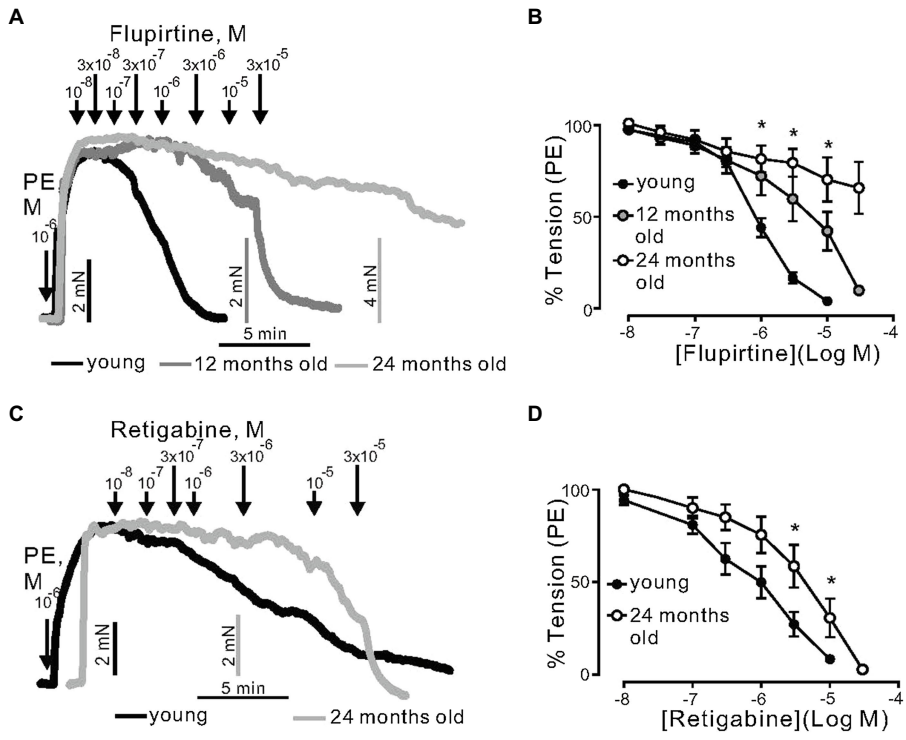

FIGURE 2 | Relaxation of (–) PVAT mesenteric artery rings by KCNQ channels activators flupirtine and retigabine. **(A)** Representative traces showing the relaxation induced by 0.01–30 µm flupirtine in rings isolated from young, 12-months, and 24-month-old mice. Mesenteric arteries were precontracted by 1 µm phenylephrine (PE). **(B)** Concentration-response relationships for flupirtine-induced relaxation in mesenteric arteries in young ($n = 12$, $N = 3$), 12-month-old ($n = 10$, $N = 4$), and 24-month-old ($n = 9$, $N = 3$) mice. **(C)** Representative traces showing the relaxation induced by 0.01–30 µm retigabine in rings isolated from young, 12-, and 24-month-old mice. **(D)** Concentration-response relationships for retigabine-induced relaxation in mesenteric arteries in young ($n = 12$, $N = 3$), and 24-month-old ($n = 7$, $N = 2$) mice. *$p < 0.05$. Two-way ANOVA followed by Tukey *post hoc* test. Data are mean and SEM.

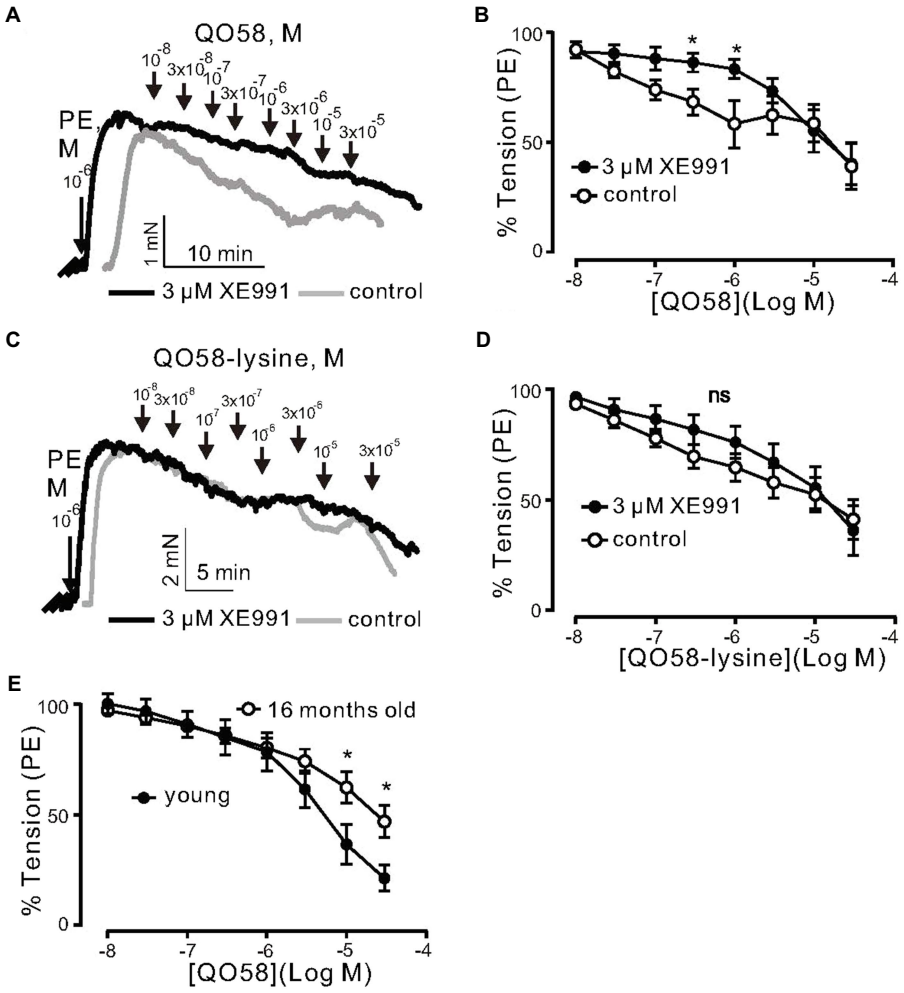

FIGURE 3 | Relaxation of (–) PVAT mesenteric artery rings by novel KCNQ channel openers QO58 and QO58-lysine. **(A)** Original traces showing the effects of 3 µM XE991 on QO58-induced relaxation in (–) PVAT mesenteric artery rings compared with control rings without XE991. **(B)** Concentration-response relationships for QO58-induced relaxation in (–) PVAT mesenteric arteries from young wild-type animals after pre-incubation with 3 µm XE991 ($n = 10$, $N = 4$) or in the absence of XE991 ($n = 6$, $N = 3$). **(C)** Original traces showing the effects of 3 µm XE991 on QO58-lysine-induced relaxation in (–) PVAT mesenteric artery rings compared with control rings without XE991. **(D)** Concentration-response relationships for QO58-lysine-induced relaxation in (–) PVAT mesenteric arteries from young animals after pre-incubation with 3 µm XE991 ($n = 10$, $N = 4$) or in the absence of XE991 ($n = 9$, $N = 3$). **(E)** Concentration-response relationships for QO58-induced relaxation in mesenteric arteries in young ($n = 11$, $N = 2$) and 16-month-old ($n = 13$, $N = 2$) mice. *$p < 0.05$. Unpaired *t* test. Data are mean and SEM.

RNA sequencing (RNA-seq) utilizing arterial tissue from young and old mice. Per sample, we obtained 23 ± 2.5 million reads. ~97,5% of all reads were mapped to the reference mouse genome (ensembl_mus_musculus_grcm38_p6_gca_000001635_8). The principal component analysis (PCA) demonstrated tight clustering within each group and transcriptome difference between groups (**Figure 5A**). In (−) PVAT mesenteric arteries isolated from 12–16-, and 24-month-old mice, we were interested in candidate genes involved in pathways regulating KCNQ channels. **Figure 5B** shows the results. The data show that none of the genes were affected by aging. However, we found that transcripts of several ion channels were up- or downregulated in (−) PVAT mesenteric arteries during aging. The results are shown in **Figures 5C–E**. Of note, the mRNA expression of *Kcnq1,3,4,5* was normal across the different ages. We also confirmed these results using qPCR (**Supplementary Figure S2**). In PVAT from 12-month-old mice, 2,202 transcripts were upregulated and 1767 were downregulated (**Figure 5F**). Top 5 down- and upregulated genes are depicted on **Figure 5G**.

Metabolic and Inflammatory Pathways

Next, we performed Gene Ontology (GO) enrichment analysis using biological process (BP) terms and KEGG pathways. Our data show that aged PVAT exhibited upregulated pathways associated with inflammatory processes (e.g., GO:0002250, GO:0051249, and GO:0002764; mmu05150, mmu05152, and mmu04060; **Supplementary Table S1**). Downregulated were mostly BP and

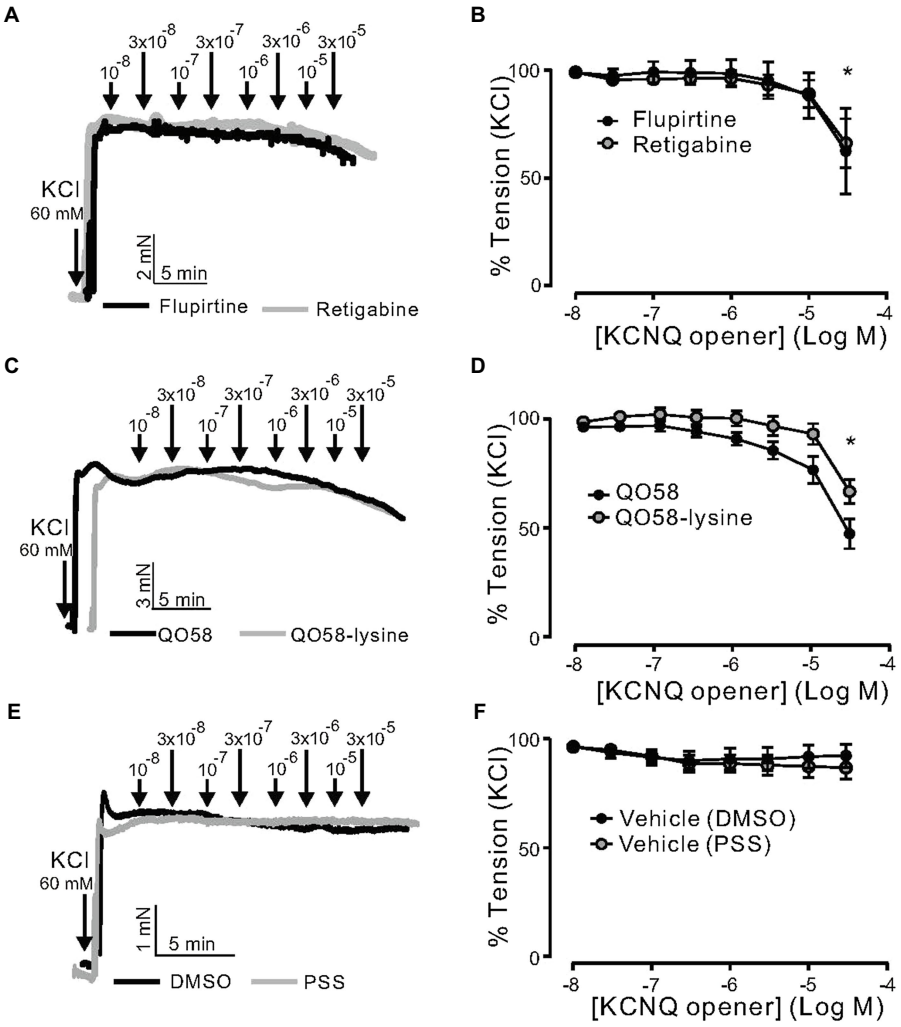

FIGURE 4 | KCNQ channel openers effects on KCl-induced contraction in (–) PVAT mesenteric artery rings. **(A)** Original recordings showing the effects of 0.01–30 μm retigabine, 0.01–30 μm flupirtine on arterial tone of isolated mesenteric artery rings without (–) PVAT. Vessels were precontracted with 60 mM KCl. **(B)** Concentration-response relationships for flupirtine- ($n = 6$, $N = 2$) and retigabine-induced relaxation ($n = 7$, $N = 2$) in (–) PVAT mesenteric arteries from young wild-type animals. **(C)** Original recordings showing the effects of 0.01–30 μm QO58 and 0.01–30 μm QO58-lysine on arterial tone of isolated mesenteric artery rings without (–) PVAT. **(D)** Concentration-response relationships for QO58 ($n = 9$, $N = 3$) and QO58-lysine-induced relaxation ($n = 8$, $N = 4$) in (–) PVAT mesenteric arteries from young wild-type animals. **(E)** Original recordings showing the effects of vehicle (DMSO or PSS) on arterial tone of isolated mesenteric artery rings without (–) PVAT. **(F)** Concentration-response relationships for DMSO ($n = 5$, $N = 2$) and PSS ($n = 5$, $N = 2$) in (–) PVAT mesenteric arteries from young wild-type animals. *$p < 0.05$. paired sample t test. Data are mean and SEM.

pathways related to generation of precursor metabolites and energy (e.g., GO:0006091, GO:0051186, GO:0006119, mmu00190, mmu01212, and mmu03320; **Supplementary Table S2**). In detail, the downregulated genes include mitochondrial genes associated with Parkinson (mmu05012) and Huntington (mmu05016), fatty acid metabolism (mmu01212), biosynthesis of unsaturated fatty acids (mmu01040), fatty acid elongation (mmu00062), insulin signaling (mmu04910), and PPAR pathway (mmu03320; **Figure 6**).

DISCUSSION

We present several novel findings. First, we showed that the anti-contractile effects of PVAT are impaired in mouse mesenteric arteries with increased age. Second, we observed altered functional role of K_V7 (KCNQ) channels during aging. Finally, aging-related transcriptome changes in mesenteric arteries and PVAT uncovered possible downstream targets of PVAT signaling pathway. Altogether, our results provide novel insights into cardiovascular events associated with aging.

Alterations in PVAT contribute to vascular dysfunction in obesity, hypertension, and cardiometabolic disease in animal models and humans (Greenstein et al., 2009; Galvez-Prieto et al., 2012). We found that the anticontractile effects of PVAT are diminished in mouse mesenteric arteries with increased age. In addition, we observed morphological changes of mesenteric PVAT during aging. PVAT cells from old mice were increased

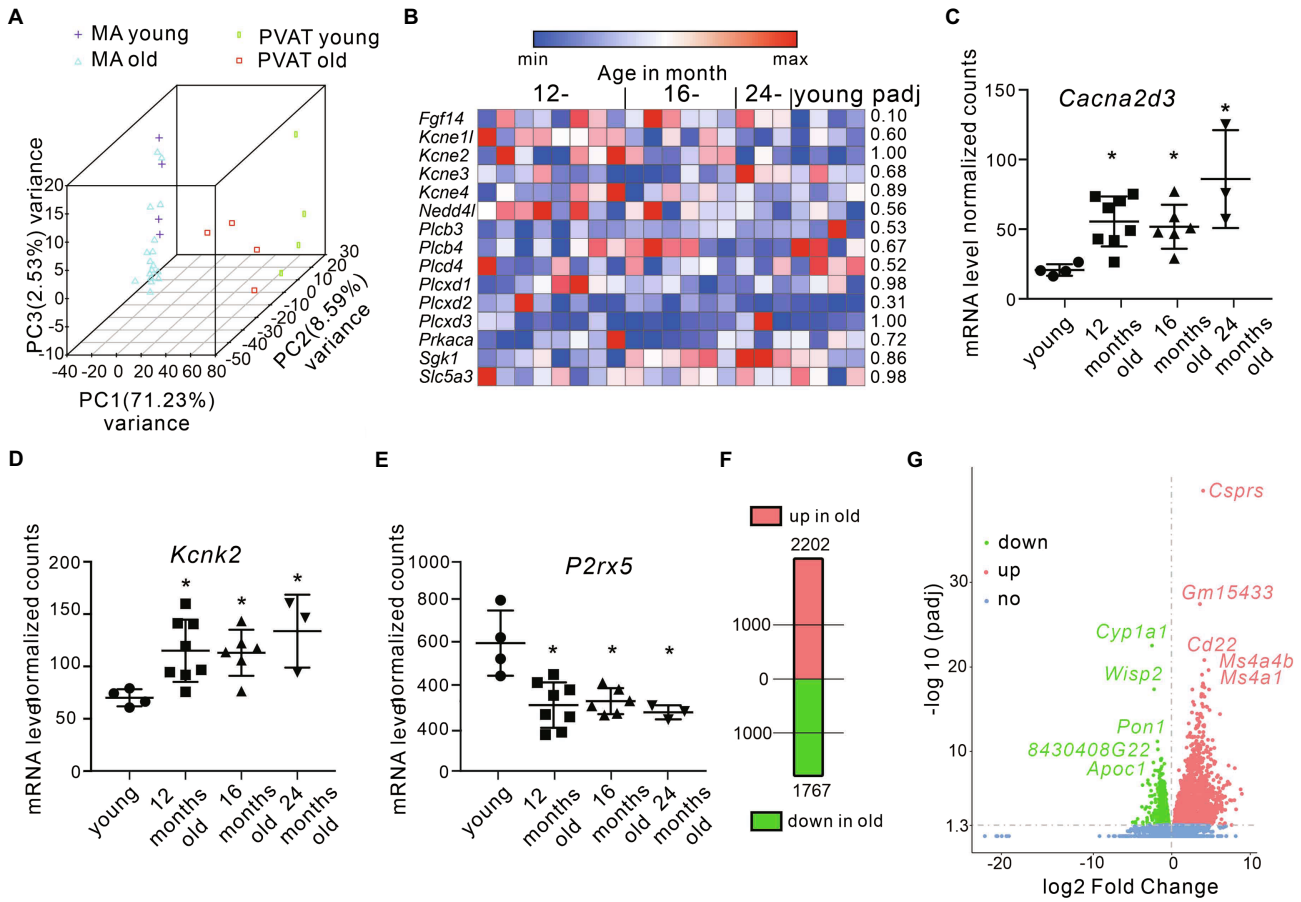

FIGURE 5 | Differential gene expression in mesenteric arteries and PVAT from young and old mice. **(A)** Principal component analysis in samples isolated from young vs. old animals. **(B)** Heatmap showing the expression of candidate genes involved in pathways regulating KCNQ channels ($N = 8$ for 12-month-old; $N = 6$ for 16-month-old; $N = 3$ for 24-month-old; $N = 4$ for young mice). Data are fragments per kilobase per million mapped fragments. **(C)** Relative mRNA levels for *Cacna2d3* ($N = 4$ for young; $N = 8$ for 12-month-old; $N = 6$ for 16-month-old; $N = 3$ for 24-month-old mice). **(D)** Relative mRNA levels for *Kcnk2* ($N = 4$ for young; $N = 8$ for 12-month-old; $N = 6$ for 16-month-old; $N = 3$ for 24-month-old mice). **(E)** Relative mRNA levels for *P2rx5* ($N = 4$ for young; $N = 8$ for 12-month-old; $N = 6$ for 16-month-old; $N = 3$ for 24-month-old mice). **(F)** Number of differentially expressed genes in PVAT isolated from mesenteric arteries in young and old mice. **(G)** Volcano plot displaying statistical significance (adjusted value of p) versus magnitude of change (fold change) for differently expressed genes in PVAT isolated from 12-month-old ($N = 4$) vs. young mice ($N = 4$). Top 5 differentially expressed genes are marked. *$p < 0.05$. Wald test. Data are mean and SD. Abbreviations can be found in **Supplementary Table S3**.

in size (**Supplementary Figure S3**). In general, hypertrophic fat cells are considered less metabolically favorable and can produce inflammatory cytokines (Stenkula and Erlanson-Albertsson, 2018). Furthermore, Ly6B inflammatory cell infiltration was higher in old PVAT (**Supplementary Figure S4**). Previous study showed that also rat aortic PVAT composition, namely, decrease of browning, is associated with vascular dysfunction during aging in spontaneous hypertensive rats (Kong et al., 2018). We conclude from these data that adipose-vascular uncoupling undergoes age-dependent changes during life span. Agabiti-Rosei et al. (2017) also found that the anticontractile effects of PVAT are abolished in mesenteric arteries from aging SAMP8 mice, which is a senescence-accelerated prone mouse model (Agabiti-Rosei et al., 2017). These findings support the notion that restoring adipose-vascular coupling could be a promising therapeutic strategy in vascular aging. We further investigated K_V7 family of K^+ channels as putative downstream targets of relaxing factors released by PVAT (Schleifenbaum et al., 2010; Tsvetkov et al., 2017). Our data show that $K_V7.3$–5 channel opening by flupirtine and retigabine induces relaxation in mesenteric arteries from young and old mice, making $K_V7.3$–5 channels a possible therapeutic target for hypertension treatment in the elderly. Similar effects were observed for QO58, which is a novel KCNQ channel activator. In whole-cell patch-clamp and cell culture experiments, QO58 demonstrates high potency of opening KCNQ channels (for $K_V7.4$ $EC_{50} = 0.6\,\mu m$, for $K_V7.3/7.5$ $EC_{50} = 5.2\,\mu m$; Zhang et al., 2013). Thus, QO58 might be a promising tool for translational research in vascular biology. Although QO58-lysine modification resulted in an improved bioavailability of the drug (Teng et al., 2016), our results in whole artery preparations argue against specificity of QO58-lysine to be capable to open KCNQ channels in intact vascular

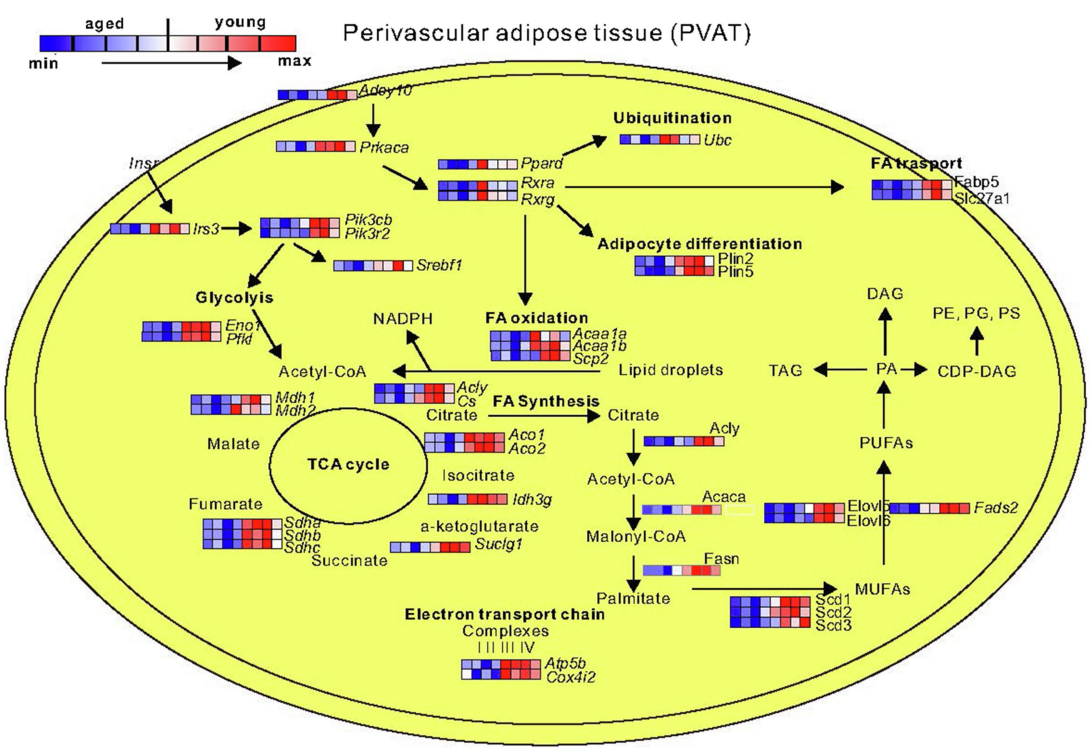

FIGURE 6 | Representative schematic of downregulated genes and pathways in PVAT isolated from mesenteric arteries of 12-month-old mice. By decreased expression of genes belonging to Ppar and Rcr signaling pathway, the ubiquitination, fatty acid (FA) transport, adipocyte differentiation, and FAs oxidation are decreased. In addition, the downregulated glycolysis, TCA cycle, and fatty acid biosynthesis can decrease production of perivascular fat tissue-derived relaxation factors ($N = 4$ for young; $N = 4$ for 12-month-old). MUFAs, monounsaturated fatty acids; PUFAs, polyunsaturated fatty acids; PA, phosphatidic acid; TAG, triacylglycerol; DAG, diacylglycerol; PE, phosphatidylethanolamine; PG, phosphatidylglycerol; PS, phosphatidylserine. Abbreviations can be found in **Supplementary Table S4**.

tissue. Nevertheless, our data demonstrate that KCNQ channel induced relaxations by the three K_V7 channel openers were more attenuated in tissue from aged mice. Moreover, electrophysiological data showed that QO58 causes hyperpolarization of the membrane potential, and this effect is reversed by XE991 in young mice. In contrast, pharmacological modulators of K_V7 channels produced no changes of membrane potential in aged mice implying that K_V7 function is altered in aging (**Figure 2; Supplementary Figure S1**). We found that *Kcnq1,3,4,5* mRNA expression was unchanged in the arteries during aging. These RNA-seq findings were confirmed by qPCR (**Supplementary Figure S2**). Thus, we concluded that impaired relaxation caused by KCNQ channels activation is not due to their changes in mRNA expression.

The RNA-Seq did not reveal additional targets or pathways. For instance, mRNA gene expressions already known to regulate KCNQ channel function (**Supplementary Table S5**) were similar in aged mice (**Figure 5B**). Thus, other mechanisms, such as post-translational modification (PTM) or trafficking, could be responsible for age-associated KCNQ channel dysfunction. Noteworthy, PTM is a new immerging paradigm of acquired channelopathies that can occur in congestive heart failure (Curran and Mohler, 2015). Post-translational modification of ion channels, such as voltage-dependent Na channels, is observed in chronic pain syndrome (Laedermann et al., 2015). Future studies are necessary to clarify PTM's contribution to regulation of vascular tone in aging.

Nonetheless, RNA-Seq revealed activation of inflammatory process in old mice in mesenteric arteries. To our knowledge, this study is the first to firmly establish inflammatory transcriptome profile during different age using small resistant arteries (diameters: 150–200 µm). Our data are also consistent with the idea that inflammation is one of the key mechanisms causing vascular damage in mouse-aged aorta (Gao et al., 2020). In addition, Th17-dependent immune response was activated (Table S1). In line with our previous findings, Th17 axis plays an important role in increased blood pressure (Wilck et al., 2017). Importantly, the anticontractile properties of PVAT can be restored in aging by melatonin treatment associated with decreased oxidative stress and inflammatory reaction (Agabiti-Rosei et al., 2017). Furthermore, anti-inflammatory therapy targeting the interleukin-1β innate immunity pathway in patients significantly decreased rate of recurrent cardiovascular events (Ridker et al., 2017). The participants were 60 years old on average and number needed to treat was relatively large (~20). Since middle-aged human (38–47 years) equivalents to 1-year-old mouse, one could argue that anti-inflammatory interventions in human should be started earlier, in order to achieve better outcome (Flurkey

et al., 2007). Moreover, in the later phase of aging, remodeling takes place as shown by upregulated GO:0030198 and extracellular matrix organization (**Supplementary Table S1**). Similar results were found in mouse aorta (Gao et al., 2020), suggesting that vasculature damage caused by low-grade inflammation is a common process in aging.

Previous studies identified NAD^+ precursor nicotinamide mononucleotide as activator of sirtuin deacylases and as a tool to reverse vascular aging (Das et al., 2018). By showing downregulation of pathway associated with energy production and therefore production of NAD and NAD precursors in mesenteric arteries of 16-month-old mice (**Supplementary Table S2**), our study contributes to the debate about the importance of NAD-dependent activity of sirtuin deacylases in aging. Interestingly, PVAT transcriptional profile in our study resembles visceral fat in insulin resistance patients. For example, downregulated mitochondrial respiratory and lipid metabolic pathways were found in obese insulin-resistant subjects (Soronen et al., 2012). We observed similar pattern in PVAT genes involved into fatty acid, cholesterol, and triglyceride metabolism (*Fatp2*, *Elovl6*, *Srebf1*). *Db/db* gene-deficient mice exhibited decreased expression of *Srebf1*, which was associated with impaired anticontractile effects of PVAT (Yahagi et al., 2002; Meijer et al., 2013). Similar results were obtained at the protein level using adipose tissue proteomic profiling in aged mice (**Supplementary Table S6**; Yu et al., 2020). The proper function of these metabolic pathways might be essential for producing PVATRFs. Although their nature is still a mystery, several proteins and lipids released by PVAT have vasodilatory properties. This state-of-affairs was previously reviewed in detail (Fernandez-Alfonso et al., 2017). Such palmitic acid methyl ester (PAME) has been proposed as transferable PVATRF in rat aorta (Lee et al., 2011). However, PAME could contribute to PVAT-induced relaxations by activating K_V7 channels in rat aorta, but not in human mesenteric arteries (Wang et al., 2018). Interestingly, omega 3 epoxide of docosahexaenoic acid (DHA) can open two-pore domain K+ channels and lower blood pressure (Nielsen et al., 2013; Ulu et al., 2014). However, whether it is indeed a PVATRF remains to be clarified. Similar metabolic pathways may control smooth muscle cell differentiation through subset of PVAT-derived stem cells (Gu et al., 2019). Thus, in addition to existing criteria such as Ca^{2+} dependence for PVATRFs, these factors could represent metabolites of fatty acids biosynthesis. Consequently, PVATRFs concentration should decrease during aging. Furthermore, PPAR pathway is compromised through peroxisome proliferator-activated receptor-γ coactivator-1 α (Ppargc1a) and lead to vascular remodeling during aging *via* decreased brown adipogenic differentiation in PVAT isolated from aorta (Pan et al., 2019). Our data indicate that PPAR pathway is also downregulated in PVAT surrounding mouse mesenteric arteries. However, the mechanism does unlikely involve *Ppargc1a* mRNA, since its expression was similar in aged and young mice (fold change = 0.27, padj = 0.47). A functionally distinct vessel type could explain this difference.

We studied mRNA transcript differences of several ion channels in aging vessels. Only three transcripts, namely, upregulated *Cacna2d3*, *Kcnk2* and downregulated *P2rx5,* intersected all three data sets (12-, 16-, and 24-month-old mice). We speculate that these ion channels could represent novel putative targets of arterial tone regulation. For example, auxiliary voltage-dependent calcium channel subunits delta (Cacna2d) contribute to trafficking and proper surface expression of voltage-gated calcium channels (VGCCs, Ca_V2; Dolphin, 2012). These channels are responsible for the P/Q current in and therefore could be of great importance for blood pressure regulation (Andreasen et al., 2006). Interestingly, *Cacna2d3 knock out* mice exhibit reduced L-type and N-type currents in spiral ganglion neurons (Stephani et al., 2019). Thus, although the vascular phenotype of *Cacna2d3*-deficient mice is not yet characterized, *Cacna2d3* arises as a novel candidate for increased blood pressure during aging. *Kcnk2* is known as TREK-1 (tandem of P domains in a weak inward-rectifier-related K^+) channel. The channel has been implicated to play an important role in the brain vasculature (Blondeau et al., 2007). TREK-1 opening characteristics (e.g., activation by PUFAs) elevates the family as possible new targets for PVATRFs. Of note, TREK-1-deficient mice display endothelial dysfunction with decreased relaxation of mesenteric arteries (Garry et al., 2007). However, the anticontractile effect of PVAT has remained to be studied in these mice. *P2rx5* is a purinoceptor for ATP acting as ligand-gated ion channel. Vascular smooth muscle cells from mesenteric arteries express the P2X receptors. Though no evidence was found for a phenotype corresponding to homomeric P2X5 receptors or to heteromeric P2X1/5 receptors, the functional role of these receptors in arteries is still unclear (Lewis and Evans, 2000). Under inflammatory conditions, osteoclasts of P2rx5 gene-deficient mice have deficits in inflammasome activation and osteoclast maturation (Kim et al., 2017). However, their vascular phenotype has not yet been studied.

DATA AVAILABILITY STATEMENT

The data presented in the study are deposited in the figshare repository, accession number 16920589 https://figshare.com/articles/dataset/raw_data_of_Aging_Affects_KV7_Channels_and_Perivascular_Adipose_Tissue-Mediated_Vascular_Tone/16920589.

ETHICS STATEMENT

The animal study was reviewed and approved by Landesamt für Gesundheit 69 und Soziales Berlin, LAGeSo. Animal care was followed by American Physiological Society guidelines, and local authorities.

AUTHOR CONTRIBUTIONS

YW, FY, AS, MK, LM, MK, FCL, MG, and DT were responsible for data collection, analysis, and interpretation. YW and DT

drafted the manuscript. All authors have approved the final version of the manuscript and agreed to be accountable for all aspects of the work. All persons designated as authors qualify for authorship, and all those who qualify for authorship are listed.

FUNDING

This work was supported by Deutsche Forschungsgemeinschaft (DFG, grant no 193179237); Deutsche Akademische Austauschdienst (DAAD); Chinese Scholarship Council.

ACKNOWLEDGMENTS

We thank Fan Zhang, Kewei Wang, Hi-lin Zhang for providing QO58-lysine and Zhihuang Zheng for assistance with quantitative real-time PCR.

SUPPLEMENTARY MATERIAL

The Supplementary Material for this article can be found online at: https://www.frontiersin.org/articles/10.3389/fphys.2021.749709/full#supplementary-material

REFERENCES

Agabiti-Rosei, C., Favero, G., De Ciuceis, C., Rossini, C., Porteri, E., Rodella, L. F., et al. (2017). Effect of long-term treatment with melatonin on vascular markers of oxidative stress/inflammation and on the anticontractile activity of perivascular fat in aging mice. *Hypertens. Res.* 40, 41–50. doi: 10.1038/hr.2016.103

Anders, S., and Huber, W. (2010). Differential expression analysis for sequence count data. *Genome Biol.* 11:R106. doi: 10.1186/gb-2010-11-10-r106

Andreasen, D., Friis, U. G., Uhrenholt, T. R., Jensen, B. L., Skott, O., and Hansen, P. B. (2006). Coexpression of voltage-dependent calcium channels Cav1.2, 2.1a, and 2.1b in vascular myocytes. *Hypertension* 47, 735–741. doi: 10.1161/01.HYP.0000203160.80972.47

Barrese, V., Stott, J. B., and Greenwood, I. A. (2018). KCNQ-encoded potassium channels as therapeutic targets. *Annu. Rev. Pharmacol. Toxicol.* 58, 625–648. doi: 10.1146/annurev-pharmtox-010617-052912

Blondeau, N., Petrault, O., Manta, S., Giordanengo, V., Gounon, P., Bordet, R., et al. (2007). Polyunsaturated fatty acids are cerebral vasodilators via the TREK-1 potassium channel. *Circ. Res.* 101, 176–184. doi: 10.1161/CIRCRESAHA.107.154443

Collaborators, G. B. D. R. F. (2020). Global burden of 87 risk factors in 204 countries and territories, 1990-2019: a systematic analysis for the global burden of disease study 2019. *Lancet* 396, 1223–1249. doi: 10.1016/S0140-6736(20)30752-2

Curran, J., and Mohler, P. J. (2015). Alternative paradigms for ion channelopathies: disorders of ion channel membrane trafficking and posttranslational modification. *Annu. Rev. Physiol.* 77, 505–524. doi: 10.1146/annurev-physiol-021014-071838

Das, A., Huang, G. X., Bonkowski, M. S., Longchamp, A., Li, C., Schultz, M. B., et al. (2018). Impairment of an endothelial NAD(+)-H2S signaling network is a reversible cause of vascular aging. *Cell* 173, 74–89. doi: 10.1016/j.cell.2018.02.008

Dolphin, A. C. (2012). Calcium channel auxiliary alpha2delta and beta subunits: trafficking and one step beyond. *Nat. Rev. Neurosci.* 13, 542–555. doi: 10.1038/nrn3311

Dupont, J. J., Mccurley, A., Davel, A. P., Mccarthy, J., Bender, S. B., Hong, K., et al. (2016). Vascular mineralocorticoid receptor regulates microRNA-155 to promote vasoconstriction and rising blood pressure with aging. *JCI Insight* 1:e88942. doi: 10.1172/2Fjci.insight.88942

Essin, K., Welling, A., Hofmann, F., Luft, F. C., Gollasch, M., and Moosmang, S. (2007). Indirect coupling between Cav1.2 channels and ryanodine receptors to generate Ca^{2+} sparks in murine arterial smooth muscle cells. *J. Physiol.* 584, 205–219. doi: 10.1113/jphysiol.2007.138982

European Medicines Agency (2018). Withdrawal of pain medicine flupirtine endorsed. Available at: https://www.ema.europa.eu/en/news/withdrawal-pain-medicine-flupirtine-endorsed

FDA (2013). *FDA Determines 2013 Labeling Adequate to Manage Risk of Retinal Abnormalities, Potential Vision Loss, and Skin Discoloration with Anti-Seizure Drug Potiga (Ezogabine)*. United States: FDA Drug Safety Communication.

Fernandez-Alfonso, M. S., Somoza, B., Tsvetkov, D., Kuczmanski, A., Dashwood, M., and Gil-Ortega, M. (2017). Role of perivascular adipose tissue in health and disease. *Compr. Physiol.* 8, 23–59. doi: 10.1002/cphy.c170004

Flurkey, K., Currer, M. J., and Harrison, D. E. (2007). "Chapter 20- Mouse Models in Aging Research," in *The Mouse in Biomedical Research. 2nd Edn.* eds. J. G. Fox, M. T. Davisson, F. W. Quimby, S. W. Barthold, C. E. Newcomer and A. L. Smith (Burlington: Academic Press), 637–672.

Galvez-Prieto, B., Somoza, B., Gil-Ortega, M., Garcia-Prieto, C. F., De Las Heras, A. I., Gonzalez, M. C., et al. (2012). Anticontractile effect of perivascular adipose tissue and Leptin are reduced in hypertension. *Front. Pharmacol.* 3:103. doi: 10.3389/fphar.2012.00103

Gao, P., Gao, P., Choi, M., Chegireddy, K., Slivano, O. J., Zhao, J., et al. (2020). Transcriptome analysis of mouse aortae reveals multiple novel pathways regulated by aging. *Aging (Albany NY)* 12, 15603–15623. doi: 10.18632/aging.103652

Garry, A., Fromy, B., Blondeau, N., Henrion, D., Brau, F., Gounon, P., et al. (2007). Altered acetylcholine, bradykinin and cutaneous pressure-induced vasodilation in mice lacking the TREK1 potassium channel: the endothelial link. *EMBO Rep.* 8, 354–359. doi: 10.1038/sj.embor.7400916

Gollasch, M. (2017). Adipose-vascular coupling and potential therapeutics. *Annu. Rev. Pharmacol. Toxicol.* 57, 417–436. doi: 10.1146/annurev-pharmtox-010716-104542

Greenstein, A. S., Khavandi, K., Withers, S. B., Sonoyama, K., Clancy, O., Jeziorska, M., et al. (2009). Local inflammation and hypoxia abolish the protective anticontractile properties of perivascular fat in obese patients. *Circulation* 119, 1661–1670. doi: 10.1161/CIRCULATIONAHA.108.821181

Gu, W., Nowak, W. N., Xie, Y., Le Bras, A., Hu, Y., Deng, J., et al. (2019). Single-cell RNA-sequencing and metabolomics analyses reveal the contribution of perivascular adipose tissue stem cells to vascular remodeling. *Arterioscler. Thromb. Vasc. Biol.* 39, 2049–2066. doi: 10.1161/ATVBAHA.119.312732

Jepps, T. A., Chadha, P. S., Davis, A. J., Harhun, M. I., Cockerill, G. W., Olesen, S. P., et al. (2011). Downregulation of Kv7.4 channel activity in primary and secondary hypertension. *Circulation* 124, 602–611. doi: 10.1161/CIRCULATIONAHA.111.032136

Jia, C., Qi, J., Zhang, F., Mi, Y., Zhang, X., Chen, X., et al. (2011). Activation of KCNQ2/3 potassium channels by novel pyrazolo[1,5-a]pyrimidin-7(4H)-one derivatives. *Pharmacology* 87, 297–310. doi: 10.1159/000327384

Kim, H., Walsh, M. C., Takegahara, N., Middleton, S. A., Shin, H. I., Kim, J., et al. (2017). The purinergic receptor P2X5 regulates inflammasome activity and hyper-multinucleation of murine osteoclasts. *Sci. Rep.* 7, 196. doi: 10.1038/s41598-017-00139-2

Kong, L. R., Zhou, Y. P., Chen, D. R., Ruan, C. C., and Gao, P. J. (2018). Decrease of perivascular adipose tissue Browning is associated With vascular dysfunction in spontaneous hypertensive rats During aging. *Front. Physiol.* 9:400. doi: 10.3389/fphys.2018.00400

Laedermann, C. J., Abriel, H., and Decosterd, I. (2015). Post-translational modifications of voltage-gated sodium channels in chronic pain syndromes. *Front. Pharmacol.* 6:263. doi: 10.3389/fphar.2015.00263

Lee, Y. C., Chang, H. H., Chiang, C. L., Liu, C. H., Yeh, J. I., Chen, M. F., et al. (2011). Role of perivascular adipose tissue-derived methyl palmitate in vascular tone regulation and pathogenesis of hypertension. *Circulation* 124, 1160–1171. doi: 10.1161/CIRCULATIONAHA.111.027375

Lewis, C. J., and Evans, R. J. (2000). Lack of run-down of smooth muscle P2X receptor currents recorded with the amphotericin permeabilized patch technique, physiological and pharmacological characterization of the properties

of mesenteric artery P2X receptor ion channels. *Br. J. Pharmacol.* 131, 1659–1666. doi: 10.1038/sj.bjp.0703744

Lohn, M., Dubrovska, G., Lauterbach, B., Luft, F. C., Gollasch, M., and Sharma, A. M. (2002). Periadventitial fat releases a vascular relaxing factor. *FASEB J.* 16, 1057–1063. doi: 10.1096/fj.02-0024com

Mani, B. K., Robakowski, C., Brueggemann, L. I., Cribbs, L. L., Tripathi, A., Majetschak, M., et al. (2016). Kv7.5 Potassium Channel subunits are the primary targets for PKA-dependent enhancement of vascular smooth muscle Kv7 currents. *Mol. Pharmacol.* 89, 323–334. doi: 10.1124/mol.115.101758

Meijer, R. I., Bakker, W., Alta, C. L., Sipkema, P., Yudkin, J. S., Viollet, B., et al. (2013). Perivascular adipose tissue control of insulin-induced vasoreactivity in muscle is impaired in db/db mice. *Diabetes* 62, 590–598. doi: 10.2337/db11-1603

Morales-Cano, D., Moreno, L., Barreira, B., Pandolfi, R., Chamorro, V., Jimenez, R., et al. (2015). Kv7 channels critically determine coronary artery reactivity: left-right differences and down-regulation by hyperglycaemia. *Cardiovasc. Res.* 106, 98–108. doi: 10.1093/cvr/cvv020

Nielsen, G., Wandall-Frostholm, C., Sadda, V., Olivan-Viguera, A., Lloyd, E. E., Bryan, R. M. Jr., et al. (2013). Alterations of N-3 polyunsaturated fatty acid-activated K2P channels in hypoxia-induced pulmonary hypertension. *Basic Clin. Pharmacol. Toxicol.* 113, 250–258. doi: 10.1111/bcpt.12092

North, B. J., and Sinclair, D. A. (2012). The intersection between aging and cardiovascular disease. *Circ. Res.* 110, 1097–1108. doi: 10.1161/CIRCRESAHA.111.246876

Pan, X. X., Ruan, C. C., Liu, X. Y., Kong, L. R., Ma, Y., Wu, Q. H., et al. (2019). Perivascular adipose tissue-derived stromal cells contribute to vascular remodeling during aging. *Aging Cell* 18:e12969. doi: 10.1111/acel.12969

Ridker, P. M., Everett, B. M., Thuren, T., Macfadyen, J. G., Chang, W. H., Ballantyne, C., et al. (2017). Antiinflammatory therapy with Canakinumab for atherosclerotic disease. *N. Engl. J. Med.* 377, 1119–1131. doi: 10.1056/NEJMoa1707914

Schleifenbaum, J., Kohn, C., Voblova, N., Dubrovska, G., Zavarirskaya, O., Gloe, T., et al. (2010). Systemic peripheral artery relaxation by KCNQ channel openers and hydrogen sulfide. *J. Hypertens.* 28, 1875–1882. doi: 10.1097/HJH.0b013e32833c20d5

Soronen, J., Laurila, P. P., Naukkarinen, J., Surakka, I., Ripatti, S., Jauhiainen, M., et al. (2012). Adipose tissue gene expression analysis reveals changes in inflammatory, mitochondrial respiratory and lipid metabolic pathways in obese insulin-resistant subjects. *BMC Med. Genet.* 5:9. doi: 10.1186/1755-8794-5-9

Stenkula, K. G., and Erlanson-Albertsson, C. (2018). Adipose cell size: importance in health and disease. *Am. J. Physiol. Regul. Integr. Comp. Physiol.* 315, R284–R295. doi: 10.1152/ajpregu.00257.2017

Stephani, F., Scheuer, V., Eckrich, T., Blum, K., Wang, W., Obermair, G. J., et al. (2019). Deletion of the Ca(2+) channel subunit alpha2delta3 differentially affects Cav2.1 and Cav2.2 currents in cultured spiral ganglion neurons Before and After the onset of hearing. *Front cell Neurosci* 13:278. doi: 10.3389/fncel.2019.00278

Tabula Muris, C. (2020). A single-cell transcriptomic atlas characterizes ageing tissues in the mouse. *Nature* 583, 590–595. doi: 10.1038/s41586-020-2496-1

Teng, B. C., Song, Y., Zhang, F., Ma, T. Y., Qi, J. L., Zhang, H. L., et al. (2016). Activation of neuronal Kv7/KCNQ/M-channels by the opener QO58-lysine and its anti-nociceptive effects on inflammatory pain in rodents. *Acta Pharmacol. Sin.* 37, 1054–1062. doi: 10.1038/aps.2016.33

Tsvetkov, D., Kassmann, M., Tano, J. Y., Chen, L., Schleifenbaum, J., Voelkl, J., et al. (2017). Do KV 7.1 channels contribute to control of arterial vascular tone? *Br. J. Pharmacol.* 174, 150–162. doi: 10.1111/bph.13665

Ulu, A., Stephen Lee, K. S., Miyabe, C., Yang, J., Hammock, B. G., Dong, H., et al. (2014). An omega-3 epoxide of docosahexaenoic acid lowers blood pressure in angiotensin-II-dependent hypertension. *J. Cardiovasc. Pharmacol.* 64, 87–99. doi: 10.1097/FJC.0000000000000094

Verlohren, S., Dubrovska, G., Tsang, S. Y., Essin, K., Luft, F. C., Huang, Y., et al. (2004). Visceral periadventitial adipose tissue regulates arterial tone of mesenteric arteries. *Hypertension* 44, 271–276. doi: 10.1161/01.HYP.0000140058.28994.ec

Vollset, S. E., Goren, E., Yuan, C. W., Cao, J., Smith, A. E., Hsiao, T., et al. (2020). Fertility, mortality, migration, and population scenarios for 195 countries and territories from 2017 to 2100: a forecasting analysis for the global burden of disease study. *Lancet* 396, 1285–1306. doi: 10.1016/S0140-6736(20)30677-2

Wang, N., Kuczmanski, A., Dubrovska, G., and Gollasch, M. (2018). Palmitic acid methyl Ester and its relation to control of tone of human visceral arteries and rat aortas by perivascular adipose tissue. *Front. Physiol.* 9:583. doi: 10.3389/fphys.2018.00583

Wilck, N., Matus, M. G., Kearney, S. M., Olesen, S. W., Forslund, K., Bartolomaeus, H., et al. (2017). Salt-responsive gut commensal modulates TH17 axis and disease. *Nature* 551, 585–589. doi: 10.1038/nature24628

Yahagi, N., Shimano, H., Hasty, A. H., Matsuzaka, T., Ide, T., Yoshikawa, T., et al. (2002). Absence of sterol regulatory element-binding protein-1 (SREBP-1) ameliorates fatty livers but not obesity or insulin resistance in Lep(Ob)/Lep(Ob) mice. *J. Biol. Chem.* 277, 19353–19357. doi: 10.1074/jbc.M201584200

Yu, G., Wang, L. G., Han, Y., and He, Q. Y. (2012). clusterProfiler: an R package for comparing biological themes among gene clusters. *OMICS* 16, 284–287. doi: 10.1089/omi.2011.0118

Yu, Q., Xiao, H., Jedrychowski, M. P., Schweppe, D. K., Navarrete-Perea, J., Knott, J., et al. (2020). Sample multiplexing for targeted pathway proteomics in aging mice. *Proc. Natl. Acad. Sci. U. S. A.* 117, 9723–9732. doi: 10.1073/pnas.1919410117

Zavaritskaya, O., Dudem, S., Ma, D., Rabab, K. E., Albrecht, S., Tsvetkov, D., et al. (2020). Vasodilation of rat skeletal muscle arteries by the novel BK channel opener GoSlo is mediated by the simultaneous activation of BK and Kv 7 channels. *Br. J. Pharmacol.* 177, 1164–1186. doi: 10.1111/bph.14910

Zhang, F., Mi, Y., Qi, J. L., Li, J. W., Si, M., Guan, B. C., et al. (2013). Modulation of K(v)7 potassium channels by a novel opener pyrazolo[1,5-a] pyrimidin-7(4H)-one compound QO-58. *Br. J. Pharmacol.* 168, 1030–1042. doi: 10.1111/j.1476-5381.2012.02232.x

Conflict of Interest: The authors declare that the research was conducted in the absence of any commercial or financial relationships that could be construed as a potential conflict of interest.

Publisher's Note: All claims expressed in this article are solely those of the authors and do not necessarily represent those of their affiliated organizations, or those of the publisher, the editors and the reviewers. Any product that may be evaluated in this article, or claim that may be made by its manufacturer, is not guaranteed or endorsed by the publisher.

SUPPLEMENTARY MATERIAL
Aging Affects K_V7 Channels and Perivascular Adipose Tissue-Mediated Vascular Tone

Figure S1.

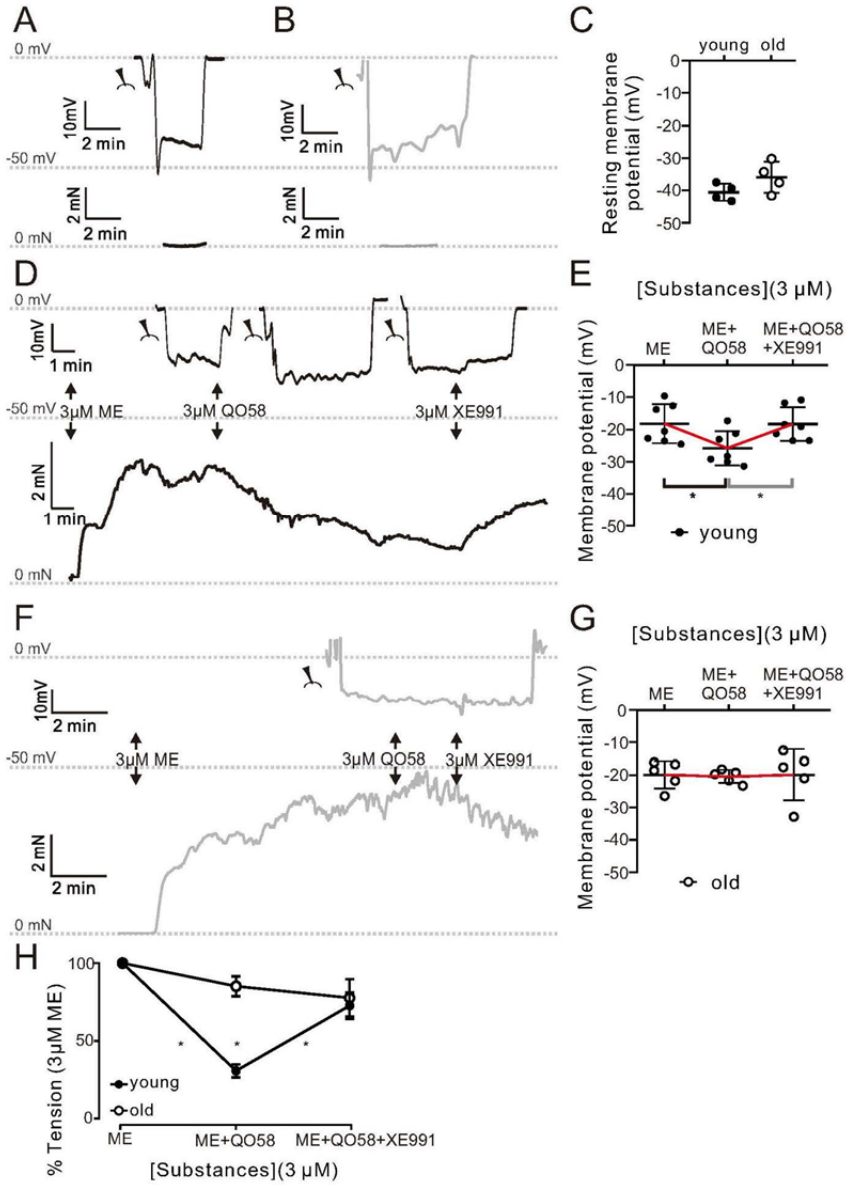

Figure S1. Aging-effects K_V7 regulation of membrane potential in mesenteric arteries

Example of resting membrane potential (upper trace) and contractile force (lower trace) in young (A) and old (B) mice. (C) Summarized data of resting membrane potential. Membrane potential (upper trace) and contractile force (lower trace) in isometric vessel preparation at 3µM methoxamine (ME)–induced tone and after subsequent application of 3 µM QO58 and 3 µM XE991 in young (D, E) and old (F, G) mice. The microelectrode symbol denotes phases when the microelectrode was impaled. Summarized data of contractile force (H) in the presence of 3µM ME, 3 µM ME + 3 µM QO58, and ME + QO58 + 3 µM XE991. (Data are mean and SD. (C): unpaired *t*-test n, N=4, for young and old mice; (E,G) *p<0.05. One-way ANOVA test with post-hoc Dunn's multiple comparison test; n=7, N=7 for young, n=5, N=5 for old mice, (H) *p<0.05. young ME vs. young ME + QO58; young ME + QO58 vs young ME+ QO58 + XE991; young ME + QO58 vs. old ME + QO58. Two-way ANOVA test with post-hoc Sidak multiple comparison test. n=7, N=7 for young, n=5, N=5 for old mice)

Figure S2.

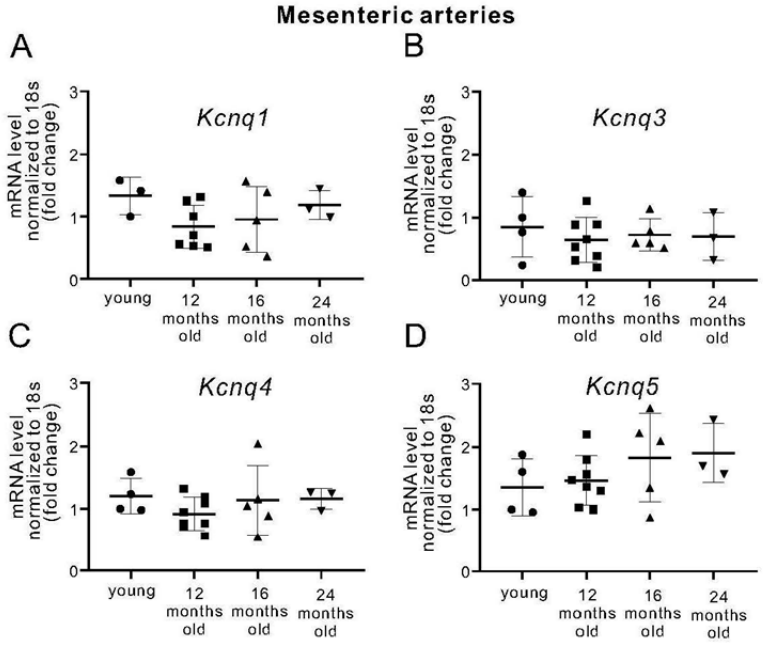

Figure S2. Relative expression of KCNQ 1, 3, 4, 5 channels at mRNA levels in (–) PVAT mesenteric arteries from young and aged mice normalized to 18s.

(A) Relative mRNA levels for Kcnq1 (N = 3 for young; N = 7 for 12-months old; N = 5 for 16-months old; N = 3 for 24 months old mice).

(B) Relative mRNA levels for Kcnq3 (N = 4 for young; N = 8 for 12-months old; N = 5 for 16-months old; N = 3 for 24-months old mice).

(C) Relative mRNA levels for Kcnq4 (N = 4 for young; N = 8 for 12-months old; N = 5, for 16-months old; N = 3 for 24-months old mice).

(D) Relative mRNA levels for Kcnq5 (N = 4 for young; N = 8 for 12-months old; N = 5 for 16-months old; N = 3 for 24-months old mice). ns, P > 0.05, Kruskal–Wallis one-way analysis of variance. Data are mean and SD.

Figure S3.

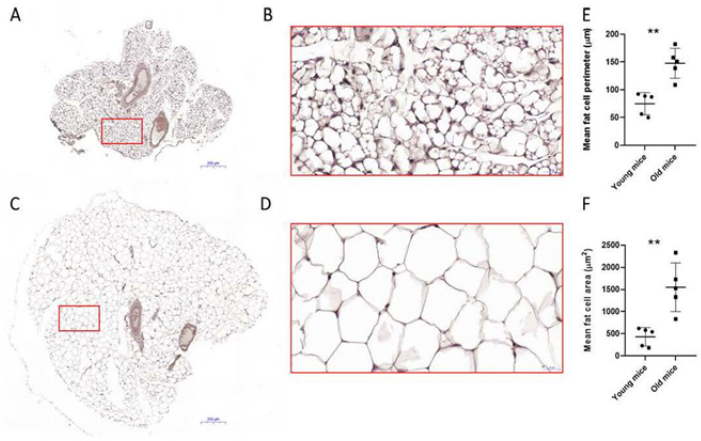

Figure S3. Age-associated changes in PVAT. Hematoxylin and eosin stain of PVAT around mesenterial arteries and veins of young (A and B) and old (C and D) mice. Mean fat cell per perimeter (C) and area (F). Magnification 5x, scale bar=200µm (A and C) and 40x, scale bar = 20µm (B and D). Data are mean and SD. *p<0.01, two-sided unpaired *t*-test.

Figure S4.

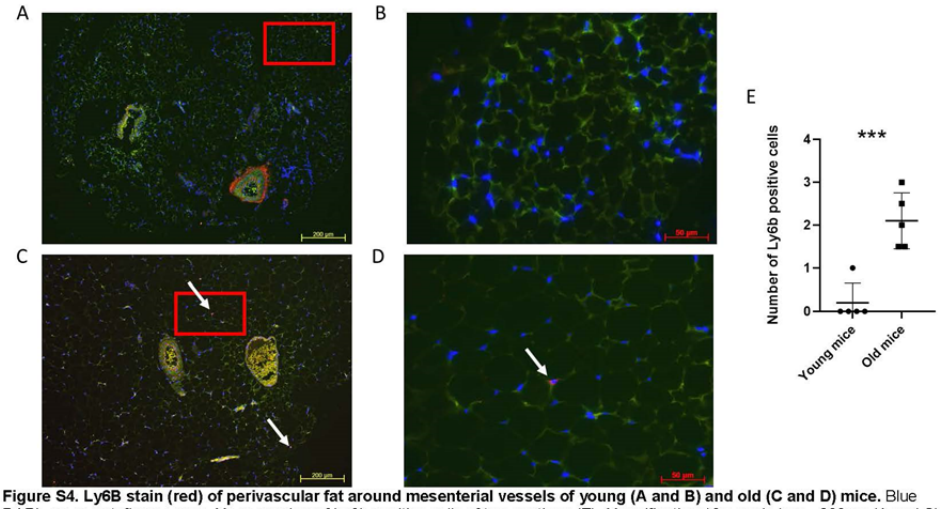

Figure S4. Ly6B stain (red) of perivascular fat around mesenterial vessels of young (A and B) and old (C and D) mice. Blue DAPI, green autofluoresence. Mean number of Ly6b positive cells of two sections (E). Magnification 10x, scale bar = 200µm (A and C) and magnification 40x, scale bar= 50 µm (B and D), ***p<0.001, two-sided unpaired t-test.

Table S1. Top upregulated GO Terms and KEGG Pathways in PVAT isolated from 12-month old mice

GO Biological Process			
id	**Terms**	**p. value**	**Adj.p.value**
GO:0002250	adaptive immune response	1.18E-90	6.11E-87
GO:0051249	regulation of lymphocyte activation	1.52E-75	3.91E-72
GO:0002764	immune response-regulating signaling pathway	5.80E-75	9.98E-72
GO:0002757	immune response-activating signal transduction	4.56E-72	5.89E-69
GO:0050867	positive regulation of cell activation	7.06E-71	7.30E-68
GO:0098542	defense response to other organism	9.32E-71	8.02E-68
GO:0002253	activation of immune response	2.83E-70	2.09E-67
GO:0002696	positive regulation of leukocyte activation	4.29E-69	2.77E-66
GO:0042113	B cell activation	1.70E-68	9.78E-66
GO:0002768	immune response-regulating cell surface receptor signaling pathway	6.12E-67	3.16E-64
GO:0051251	positive regulation of lymphocyte activation	1.54E-66	7.21E-64
GO:0002429	immune response-activating cell surface receptor signaling pathway	1.36E-64	5.85E-62
GO:0050851	antigen receptor-mediated signaling pathway	5.76E-64	2.29E-61
GO:0002460	adaptive immune response based on somatic recombination of immune receptors built from immunoglobulin superfamily domains	1.23E-63	4.53E-61
GO:0002443	leukocyte mediated immunity	2.14E-60	7.36E-58
GO:0002449	lymphocyte mediated immunity	1.72E-58	5.56E-56
GO:0050864	regulation of B cell activation	9.82E-57	2.98E-54
GO:0050853	B cell receptor signaling pathway	6.90E-56	1.98E-53
GO:0042110	T cell activation	1.30E-51	3.53E-49
GO:0002250	adaptive immune response	1.18E-90	6.11E-87
KEGG			
id	**Terms**	**p. value**	**Adj.p.value**
mmu04060	Cytokine-cytokine receptor interaction	1.35E-24	4.06E-22
mmu05340	Primary immunodeficiency	7.28E-23	1.09E-20
mmu04640	Hematopoietic cell lineage	3.45E-22	3.45E-20
mmu04672	Intestinal immune network for IgA production	2.17E-17	1.62E-15
mmu04380	Osteoclast differentiation	1.00E-16	6.02E-15
mmu04658	Th1 and Th2 cell differentiation	1.48E-16	7.42E-15
mmu05321	Inflammatory bowel disease (IBD)	2.26E-16	9.47E-15
mmu04064	NF-kappa B signaling pathway	2.52E-16	9.47E-15
mmu04650	Natural killer cell mediated cytotoxicity	3.40E-16	1.13E-14
mmu05330	Allograft rejection	1.17E-15	3.51E-14
mmu04660	T cell receptor signaling pathway	1.47E-15	4.02E-14
mmu04514	Cell adhesion molecules (CAMs)	1.82E-15	4.56E-14
mmu04659	Th17 cell differentiation	2.98E-15	6.89E-14
mmu04662	B cell receptor signaling pathway	3.09E-14	6.62E-13
mmu05332	Graft-versus-host disease	4.92E-14	9.85E-13
mmu04061	Viral protein interaction with cytokine and cytokine receptor	6.91E-14	1.30E-12
mmu05168	Herpes simplex virus 1 infection	6.48E-13	1.14E-11
mmu04940	Type I diabetes mellitus	2.12E-12	3.53E-11

mmu05140	Leishmaniasis	3.59E-12	5.67E-11
mmu04060	Cytokine-cytokine receptor interaction	1.35E-24	4.06E-22

Table S2. Top downregulated GO Terms and KEGG Pathways in PVAT isolated from 12-month old mice

GO Biological Process			
id	**Terms**	**p. value**	**Adj.p.value**
GO:0006091	generation of precursor metabolites and energy	7.32E-47	3.48E-43
GO:0051186	cofactor metabolic process	4.73E-41	1.12E-37
GO:0022900	electron transport chain	2.51E-39	3.98E-36
GO:0045333	cellular respiration	9.33E-39	1.11E-35
GO:0046034	ATP metabolic process	1.84E-36	1.75E-33
GO:0032787	monocarboxylic acid metabolic process	7.77E-36	6.15E-33
GO:0015980	energy derivation by oxidation of organic compounds	9.13E-35	6.20E-32
GO:0009161	ribonucleoside monophosphate metabolic process	4.17E-34	2.48E-31
GO:0009167	purine ribonucleoside monophosphate metabolic process	6.48E-34	3.42E-31
GO:0006119	oxidative phosphorylation	7.45E-34	3.54E-31
GO:0009199	ribonucleoside triphosphate metabolic process	8.44E-34	3.65E-31
GO:0009126	purine nucleoside monophosphate metabolic process	9.63E-34	3.81E-31
GO:0009205	purine ribonucleoside triphosphate metabolic process	2.11E-33	7.73E-31
GO:0009144	purine nucleoside triphosphate metabolic process	3.64E-33	1.23E-30
GO:0009123	nucleoside monophosphate metabolic process	6.08E-33	1.93E-30
GO:0022904	respiratory electron transport chain	1.38E-32	4.11E-30
GO:0009141	nucleoside triphosphate metabolic process	4.63E-32	1.29E-29
GO:0007005	mitochondrion organization	4.26E-31	1.12E-28
GO:0042773	ATP synthesis coupled electron transport	1.32E-30	3.30E-28
GO:0042775	mitochondrial ATP synthesis coupled electron transport	2.14E-30	5.08E-28
KEGG			
id	**Terms**	**p. value**	**Adj.p.value**
mmu05012	Parkinson disease	1.23E-41	3.79E-39
mmu00190	Oxidative phosphorylation	7.22E-41	1.11E-38
mmu05016	Huntington disease	3.95E-33	3.64E-31
mmu04932	Non-alcoholic fatty liver disease (NAFLD)	4.74E-33	3.64E-31
mmu04714	Thermogenesis	1.07E-30	6.59E-29
mmu01200	Carbon metabolism	9.08E-19	4.64E-17
mmu01212	Fatty acid metabolism	3.19E-18	1.40E-16
mmu04723	Retrograde endocannabinoid signaling	8.22E-15	3.16E-13
mmu04146	Peroxisome	2.66E-11	9.07E-10
mmu00620	Pyruvate metabolism	3.06E-11	9.40E-10
mmu03320	PPAR signaling pathway	3.68E-11	1.03E-09
mmu00020	Citrate cycle (TCA cycle)	2.73E-10	6.99E-09
mmu00280	Valine, leucine and isoleucine degradation	4.99E-10	1.18E-08
mmu00010	Glycolysis / Gluconeogenesis	2.95E-09	6.34E-08
mmu04260	Cardiac muscle contraction	3.10E-09	6.34E-08
mmu01040	Biosynthesis of unsaturated fatty acids	7.96E-09	1.53E-07

mmu01230	Biosynthesis of amino acids	4.98E-08	8.99E-07
mmu00062	Fatty acid elongation	6.78E-08	1.16E-06
mmu00640	Propanoate metabolism	3.46E-07	5.58E-06
mmu00900	Terpenoid backbone biosynthesis	5.77E-07	8.86E-06

Table S3. Abbreviations used in Figure 5

Gene Symbol	Gene Description
Fgf14	Fibroblast growth factor 14
Kcne1l	Potassium voltage-gated channel subfamily E regulatory beta subunit 5
Kcne2	Potassium voltage-gated channel subfamily E Isk-related subfamily 2
Kcne3	Potassium voltage-gated channel subfamily E member 3
Kcne4	Potassium voltage-gated channel subfamily E member 4
Nedd4l	Neural precursor cell expressed, developmentally down-regulated 4-like, E3 ubiquitin protein ligase
Plcb3	phospholipase C, beta 3
Plcb4	phospholipase C, beta 4
Plcd4	phospholipase C, delta 4
Plcxd1	PI-PLC X domain-containing protein 1
Plcxd2	PI-PLC X domain-containing protein 2
Plcxd3	Phosphatidylinositol-specific phospholipase C, X domain containing 3
Prkaca	protein kinase, cAMP dependent, catalytic, alpha
Sgk1	Serine/threonine-protein kinase Sgk1
Slc5a3	Sodium/myo-inositol cotransporter
Cyp1a1	Cytochrome P450 1A1
Wisp2	WNT1 inducible signaling pathway protein 2
Pon1	Paraoxonase 1
8430408G22	Protein DEPP1
Apoc1	Apolipoprotein C-I Truncated apolipoprotein C-I
Csprs	Component of Sp100-rs
Gm15433	predicted pseudogene 15433
Cd22	CD22 molecule
Ms4ab	Membrane-spanning 4-domains, subfamily A, member 4B
Ms4a1	Membrane-spanning 4-domains, subfamily A, member 1

Table S4. Abbreviations used in Figure 6

Gene Symbol	Gene Description
Adcy10	Adenylate cyclase type 10
Prkaca	Protein kinase, cAMP dependent, catalytic, alpha
Ppard	Peroxisome proliferator-activated receptor delta
Rxra	Retinoid X receptor alpha
Rxrg	Retinoic acid receptor RXR-gamma
Ubc	Ubiquitin C
Fabp5	Fatty acid-binding protein
Plin2	Perilipin-2

Plin5	Perilipin-5
Acaa1a	Acetyl-Coenzyme A acyltransferase 1A
Acaa1b	Acetyl-Coenzyme A acyltransferase 1B
Scp2	Sterol carrier protein 2
Insr	Insulin receptor
Irs3	Insulin receptor substrate 3
Pik3cb	Phosphatidylinositol 4,5-bisphosphate 3-kinase catalytic subunit beta isoform
Pik3r2	Phosphatidylinositol 3-kinase regulatory subunit beta
Srebf1	Sterol regulatory element-binding protein 1
Eno1	Alpha-enolase
Pfkl	ATP-dependent 6-phosphofructokinase
Acly	ATP citrate lyase
Cs	Citrate synthase
Aco1	Aconitase 1
Aco2	Aconitase 2
Idh3g	Isocitrate dehydrogenase 3 (NAD+), gamma
Suclg1	Succinate-CoA ligase [ADP/GDP-forming] subunit alpha
Sdha	Succinate dehydrogenase complex, subunit A
Sdhb	Succinate dehydrogenase complex, subunit B
Sdhc	Succinate dehydrogenase complex, subunit C
Mdh1	Malate dehydrogenase 1
Mdh2	Malate dehydrogenase 2
Acaca	Acetyl-Coenzyme A carboxylase alpha
Fasn	Fatty acid synthase
Atp5b	ATP synthase subunit beta
Cox4i2	Cytochrome c oxidase subunit 4 isoform 2
Scd1	Acyl-CoA desaturase 1
Scd2	Acyl-CoA desaturase 2
Scd3	Acyl-CoA desaturase 3
Fads2	Fatty acid desaturase 2
Elovl5	Elongation of very long-chain fatty acid protein 5
Elovl6	Elongation of very long-chain fatty acid protein 6

Table S5. Candidates involved in pathways regulating KCNQ channels

Candidate	Effect	Reference
FGF14	Positively regulates KCNQ channels	(1)
Kcne4	Alters Vascular Reactivity through modulating KCNQ channels	(2)
PIP_2	Regulates KCNQ channel openings	(Zaydman et al., 2013
cAMP/PKA	Enhance KCNQ currents	(3)
SGK-1 and Nedd4-2	Modulates KCNQ channels by SGK-1 regulation of the activity of the ubiquitin ligase Nedd4-2	(4)
SMIT1 or Slc5a3	Regulates KCNQ channel	(5, 6)

	ion selectivity	

Table S6. Significantly dysregulated genes in PVAT (RNA-Seq) and in white adipose tissue (WAT) (proteomics) in aging.

Gene Symbol (mRNA, from current study)	Gene Symbol (proteomics from (7))	Gene description	Expression	Process
Abhd14b	Abhd14b	Abhydrolase domain containing 14b	↓	Lipid Metabolism
Abhd6	Abhd6	Abhydrolase domain containing 6	↓	
Acaca	Acaca	Acetyl-Coenzyme A carboxylase alpha	↓	
Acacb	Acacb	Acetyl-Coenzyme A carboxylase beta	↓	
Echs1	Echs1	Enoyl-CoA hydratase, mitochondrial	↓	
Fasn	Fasn	Fatty acid synthase	↓	
Gpd2	Gpd2	Pleckstrin homology domain-containing family O member 1	↓	
Acly	Acly	ATP citrate lyase	↓	Central Carbon
Gls	Gls	Glutaminase kidney isoform, mitochondrial	↑	
Hk2	Hk2	Hexokinase-2	↓	
Mcee	Mcee	Methylmalonyl-CoA epimerase, mitochondrial	↓	
Pdhb	Pdhb	Pyruvate dehydrogenase E1 component subunit beta, mitochondrial	↓	
Pgk1	Pgk1	Phosphoglycerate kinase 1	↓	
Gpt2	Gpt2	Glutamic pyruvate transaminase	↓	
Hk3	Hk3	Hexokinase-3	↑	
Cox5b		Cytochrome c oxidase subunit 5B, mitochondrial	↓	
Cox6b1	Cox6b1	Cytochrome c oxidase subunit 6B1	↓	
Cox6c	Cox6c	Cytochrome c oxidase subunit 6C	↓	
Ndufa3	Ndufa3	NADH dehydrogenase [ubiquinone] 1 alpha subcomplex subunit 3	↓	
Ndufa4	Ndufa4	NADH dehydrogenase [ubiquinone] 1 alpha	↓	

		subcomplex subunit 4		Electron Transport Chain
Ndufa5	Ndufa5	NADH dehydrogenase [ubiquinone] 1 alpha subcomplex subunit 5	↓	
Ndufa6	Ndufa6	NADH dehydrogenase [ubiquinone] 1 alpha subcomplex subunit 6	↓	
Ndufa7	Ndufa7	NADH dehydrogenase [ubiquinone] 1 alpha subcomplex subunit 7	↓	
Ndufa8	Ndufa8	NADH dehydrogenase [ubiquinone] 1 alpha subcomplex subunit 8	↓	
Ndufa10	Ndufa10	NADH dehydrogenase [ubiquinone] 1 alpha subcomplex subunit 10	↓	
Ndufa11	Ndufa11	NADH dehydrogenase [ubiquinone] 1 alpha subcomplex subunit 11	↓	
Ndufa12	Ndufa12	NADH dehydrogenase [ubiquinone] 1 alpha subcomplex subunit 12	↓	
Ndufb7	Ndufb7	NADH dehydrogenase [ubiquinone] 1 beta subcomplex subunit 7	↓	
Ndufb10	Ndufb10	NADH dehydrogenase [ubiquinone] 1 beta subcomplex subunit 10	↓	
Ndufb11	Ndufb11	NADH dehydrogenase [ubiquinone] 1 beta subcomplex subunit 11	↓	
Ndufs2	Ndufs2	NADH dehydrogenase [ubiquinone] iron-sulfur protein 2	↓	
Ndufs4	Ndufs4	NADH dehydrogenase [ubiquinone] iron-sulfur protein 4	↓	
Ndufs5	Ndufs5	NADH dehydrogenase [ubiquinone] iron-sulfur protein 5	↓	
Ndufs6	Ndufs6	NADH dehydrogenase [ubiquinone] iron-sulfur protein 6	↓	
Ndufs7	Ndufs7	NADH dehydrogenase [ubiquinone] iron-sulfur protein 7	↓	
Ndufv1	Ndufv1	NADH dehydrogenase [ubiquinone] flavoprotein 1	↓	
Ndufv2	Ndufv2	NADH dehydrogenase [ubiquinone] flavoprotein 2	↓	

Uqcrfs1	Uqcrfs1	Ubiquinol-cytochrome c reductase, Rieske iron-sulfur polypeptide 1	↓	
Casp1	Casp1	Caspase-1	↑	Inflammation
Cd68	Cd68	Macrosialin	↑	
Mrc1	Mrc1	Macrophage mannose receptor 1	↑	
Itgam	Itgam	Integrin alpha-M	↑	
Stat2	Stat2	Signal transducer and activator of transcription 2	↑	
Rnasel	Rnasel	2-5A-dependent ribonuclease	↑	

References:

1. **Pablo JL, and Pitt GS**. FGF14 is a regulator of KCNQ2/3 channels. *Proc Natl Acad Sci U S A* 114: 154-159, 2017.
2. **Abbott GW, and Jepps TA**. Kcne4 Deletion Sex-Dependently Alters Vascular Reactivity. *J Vasc Res* 53: 138-148, 2016.
3. **Mani BK, Robakowski C, Brueggemann LI, Cribbs LL, Tripathi A, Majetschak M, and Byron KL**. Kv7.5 Potassium Channel Subunits Are the Primary Targets for PKA-Dependent Enhancement of Vascular Smooth Muscle Kv7 Currents. *Mol Pharmacol* 89: 323-334, 2016.
4. **Schuetz F, Kumar S, Poronnik P, and Adams DJ**. Regulation of the voltage-gated K(+) channels KCNQ2/3 and KCNQ3/5 by serum- and glucocorticoid-regulated kinase-1. *Am J Physiol Cell Physiol* 295: C73-80, 2008.
5. **Manville RW, Neverisky DL, and Abbott GW**. SMIT1 Modifies KCNQ Channel Function and Pharmacology by Physical Interaction with the Pore. *Biophys J* 113: 613-626, 2017.
6. **Barrese V, Stott JB, Baldwin SN, Mondejar-Parreno G, and Greenwood IA**. SMIT (Sodium-Myo-Inositol Transporter) 1 Regulates Arterial Contractility Through the Modulation of Vascular Kv7 Channels. *Arterioscler Thromb Vasc Biol* 40: 2468-2480, 2020.
7. **Yu Q, Xiao H, Jedrychowski MP, Schweppe DK, Navarrete-Perea J, Knott J, Rogers J, Chouchani ET, and Gygi SP**. Sample multiplexing for targeted pathway proteomics in aging mice. *Proc Natl Acad Sci U S A* 117: 9723-9732, 2020.

9. Curriculum Vitae

My curriculum vitae does not appear in the electronic version of my paper for reasons of data protection.

My curriculum vitae does not appear in the electronic version of my paper for reasons of data protection.

My curriculum vitae does not appear in the electronic version of my paper for reasons of data protection.

10. Complete list of publications

Original Publishing

Yibin Wang, Fatima Yildiz, Andrey Struve, Mario Kassmann, Lajos Markó, May-Britt Köhler, Friedrich C. Luft, Maik Gollasch and Dmitry Tsvetkov. Aging affects K_V7 channels and perivascular-adipose tissue-mediated vascular tone. Front. Physiol., 26 November 2021; 12:749709. DOI link: https://doi.org/10.3389/fphys.2021.749709.

Impact Factor(2020/2021):4.566

Abstracts/Poster

Yibin Wang, Fatima Yildiz, Andrey Struve, Mario Kassmann, Lajos Markó, May-Britt Köhler, Friedrich C. Luft, Maik Gollasch and Dmitry Tsvetkov. Aging affects K_V7 channels and perivascular-adipose tissue-mediated vascular tone, Gesellschaft für Mikrozirkulation und Vaskuläre Biologie(Gfmvb) meeting, Goettingen, Nov 3-5, 2021: Poster

11. Acknowledgments

At this point, I would like to thank all those who have supported me during the preparation of this work.

First of all, I would like to thank my supervisor and thesis supervisor Prof. Dr. med. Dr. rer. nat. Maik Gollasch for hosting me in his lab and providing me the opportunity to do my projects. I learnt a lot from his immense knowledge, excellent supervision and enthusiasm, those really inspired me and built the basis for my passion to science that I developed throughout my studies. He gives me much help and many advices in every stages of my doctoral studying, which made all of my accomplishments possible.

Furthermore, I would like to express my thanks to Prof. Dr. Friedrich C. Luft for his adives on my research as well as my paper. And I'd like to thank Dr. Dmitry Tsvetkov for the guidance in designing the project, and the effort on the electrophysiology and RNA-seq, as well as establishing the techniques on myograph and membrane potential recordings.

I would like to particularly thank my colleagues I collaborated with and who contributed to my work: Andrey Struve, Fatima Yildiz, Gang Fan, Lajos Marko, Mario Kaßmann, Nadine Wittstruck, Tong Liu, Weiying Kong, Yingqiu Cui, Yoland Anistan, Zhihuang Zheng (in alphabetical order). They all inspired me in their own ways to become what one could call a scientist.

Finally and most importantly, I want to thank my love Yajie Zheng for encouraging me during the whole time of study. My friends and my family have always been the support for me in the toughest time.

Importantly, my thanks would go to the China Scholarship Council for financial support during my research.